Draft Environmental Impact Statement

Infrastructure Improvements at the Yap International Airport and the Yap Seaport

Yap State, Federated States of Micronesia

ID# EISX-007-USN-1775813621

APRIL 2026

Appendix P
Sediment Plume Dispersion Modeling (2026)

Naval Facilities Engineering Systems Command
NAVFAC Southwest

Plume Dispersion Modelling Report

Contract No. N62473-19-D-2432
Task Order No. N62473-23-F-4522

Yap Port and Harbor Improvements

Yap, Federated States of Micronesia

March 20 2026

GHD COWI
JOINT VENTURE

Contents

List of Figures

List of Tables

1 Introduction

The Port of Yap is located in Colonia Harbor, the capital city of Yap Island, a state in the Federated States of Micronesia (FSM). Receiving domestic and international goods, the port facilities comprise a contiguous wharf (split into two berths), two small barge slips located on the east and west ends of the primary wharf face, and a landing craft Ro-Ro (Roll-on, Roll-off) ramp south of the east barge slip. Colonia Harbor is accessed from deep water through a natural channel from the island's fringing outer reef. Channel improvement projects have previously widened and deepened the natural channel to facilitate shipping. Refer to Figure 1-1.

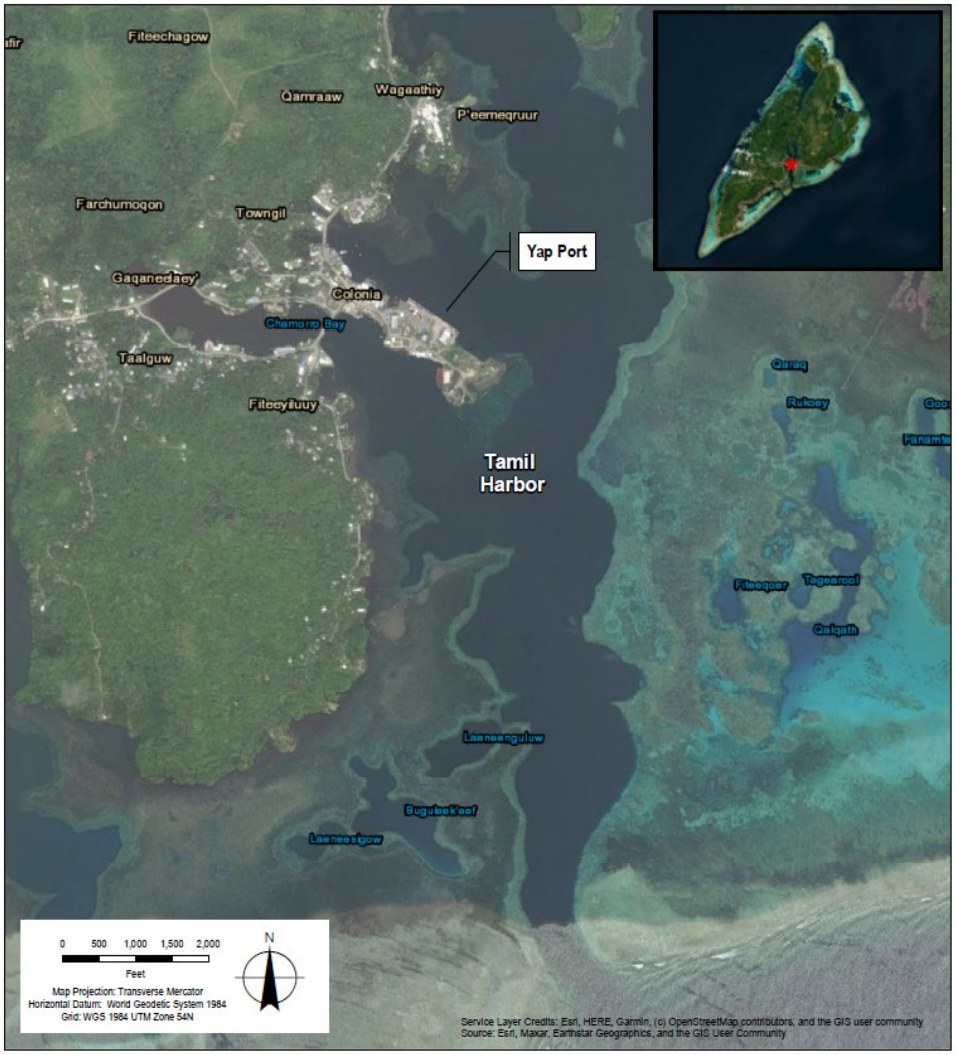

Figure 1-1 Port of Yap

1.1 Purpose of this Report

This memorandum summarizes the results of sediment plume dispersion modeling conducted for dredging activities in the navigation channels and existing berths at Yap Port. The focus is on presenting the key findings relevant to the potential increase of suspended sediment concentration (SSC) as a consequence

of the proposed dredging activity under unmitigated scenarios (meaning, for example, without turbidity barriers in place).

2 Methodology

The Danish Hydraulic Institute's (DHI) MIKE software suite was used to predict changes in SSC and sediment deposition resulting from dredging and stockpiling activities at Yap Port. The DHI MIKE software suite is globally recognized and widely accepted by regulators, industry, and academia as a suitable and industry standard numerical modelling platform for this purpose.

- The MIKE 3 Flexible Mesh Hydrodynamic (HD) model simulated three-dimensional hydrodynamics influenced by tides, wind, Coriolis force, and air pressure variations.
- The MIKE Spectral Waves (SW) module represented wave dynamics.
- Outputs from these models provided current and wave data for the MIKE 3 Mud Transport (MT) model, which simulated dispersion, deposition, and resuspension of fine sediments generated during dredging.

Further details on the modeling platform, approach and validation are provided in Sections 4 and 5. The output from the modeling is a spatial varying predicted change in SSC (often denoted as ΔSSC) from baseline, and an amount of sediment deposition within that trajectory. Baseline SSC is the amount of naturally occurring or man-made/introduced sediment load present in the marine environment to be simulated. For Yap, this could include sediment from rainfall runoff following typical seasonal weather events, or sediment generated from typical in-water activities occurring around the island. The modeling platform is capable of simulating baseline SSC and therefore calculating the change as a result of the Project activities. Unfortunately, there was no baseline data identified for this Project. Therefore, the methodology adopted in this study was to predict ΔSSC and sediment deposition against a baseline condition of zero.

2.1 Dredge Depth

The dredge design depths vary based on the underkeel clearance calculations performed for the design vessels and the transit speed, plus an overdepth allowance of 1 foot (except for the pocket dredging site at Tamil and Rull). The dredge sites are shown in Figure 2-1.

Table 2-1 Dredging Contract Depths

Dredge Area	Contract Depth (ft)	Overdepth Allowance (ft)
Berth	-36.0	-1.0
Turning Basin	-38.0	-1.0
Entrance Channel West	-40.5	-1.0
Entrance Channel East	-40.5	-1.0
Tamil (pocket entrance dredging)	-10.0	NA
Rull (pocket entrance dredging)	-10.0	NA

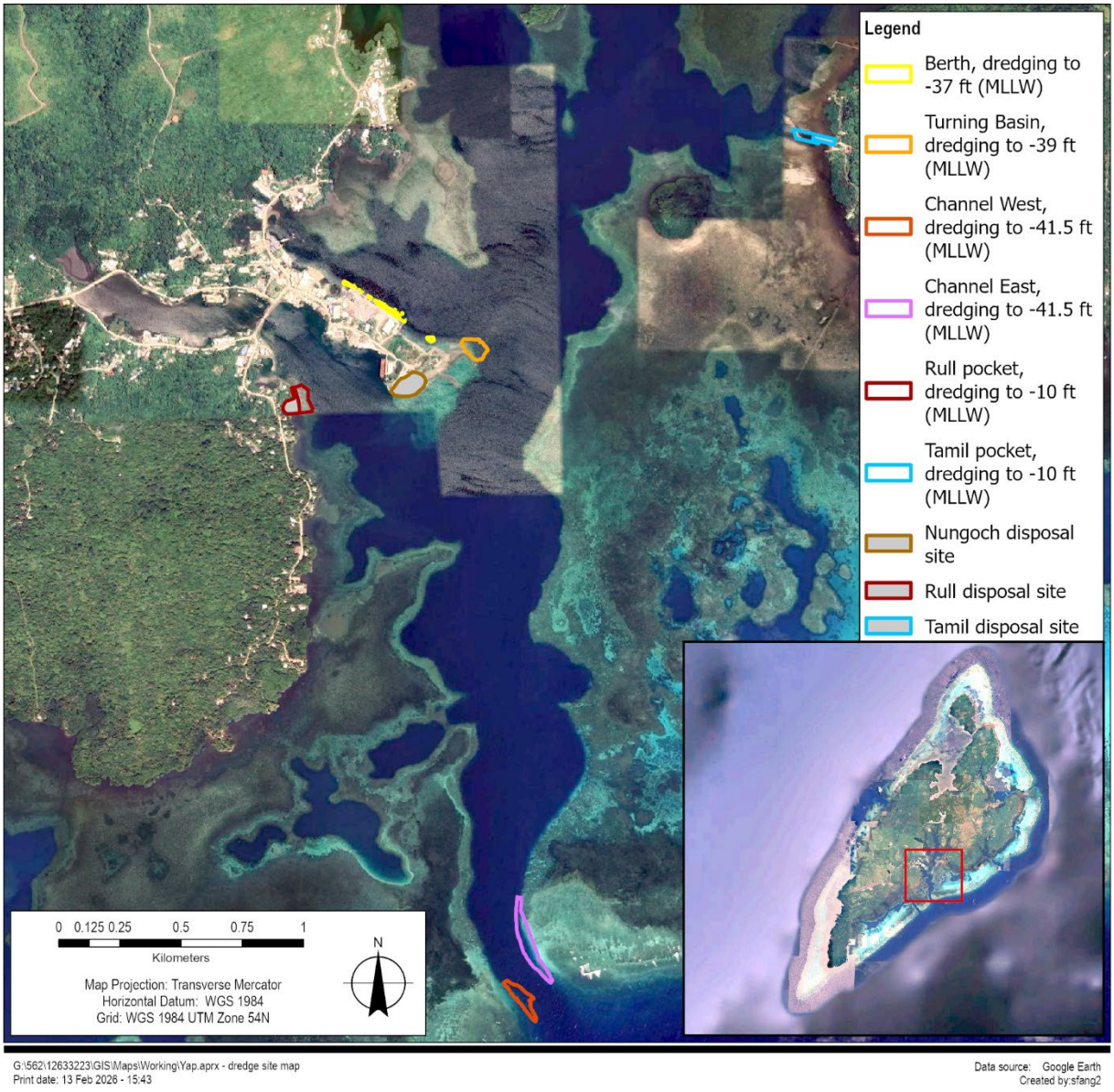

Figure 2-1 Dredge site map

2.2 Quantities of Dredge Materials

A total volume of 130,000 cubic yards (CY, equivalent to ~100,000 m^3) will be dredged from the areas. The anticipated volumes for each dredge area are tabulated in Table 2-2.

Table 2-2 Dredging Areas and Volumes

Dredge Area	Area		Volume	
	Square Feet	Square Meters	Cubic Yards	Cubic Meters
Berth	20,800	2,000	2,500	2,000
Turning Basin	64,800	6,100	25,600	19,600
Channel East	139,900	13,000	53,800	41,100
Channel West	71,500	6,700	24,000	18,400
Tamil Pocket Area			10,000	7,700
Rull Pocket Area			14,400	11,200
TOTAL	297,000	27,800	130,300	100,000

Notes:

- *Volumes are in situ and exclude bulking / losses and overdredge*
- *Volumes exclude contingencies relating to survey and model accuracy, design development, sedimentation, etc.*

2.3 Dredging Equipment

A large backhoe dredge (BHD) with two barges (with 1,500 CY capacity each) were assumed for the dredging and transport to Nungoch and Rull. Further details on the production rates, operational schedule and sediment flux are provided in Section 5.2.

3 Environmental Conditions

3.1 Water levels

Yap experiences a mixed semi-diurnal tidal cycle, meaning that there are two high tides and two low tides of differing values per lunar day. The UHSLC operates and maintains a network of tide stations throughout the Pacific Ocean. The representative tide gauge for the project site is located within Yap Harbour, approximately 850 m from the wharf (UHSLC ID 008). The station contains a data record as far back as 1969 (Caldwell et al. 2015).

UHSLC provides water level datums for each tide station, which are presented below in Table 3-1. A moderate tidal range occurs at the site, with the highest astronomical tide (HAT) reaching +1.39 meters above Mean Lower Low Water (MLLW), and lowest astronomical tide (LAT) of 1.91 meters below MLLW. Mean sea level (MSL) in the region is +0.62 meters MLLW.

Table 3-1 Water Level Datums for Yap

Datum	Water Level (m, MLLW)	Water Level (ft, MLLW)
Highest Observed Water Level (9/4/2004)	2.56	8.39
Highest Astronomical Tide (HAT) (18/9/1993)	1.39	4.55
Mean Higher-High Water (MHHW)	1.11	3.63

Mean High Water (MHW)	1.05	3.44
Mean Tide Level (MTL)	0.63	2.05
Mean Sea Level (MSL)	0.62	2.03
Mean Diurnal Tide Level (DTL)	0.56	1.82
Mean Low Water (MLW)	0.21	0.66
Mean Lower-Low Water (MLLW)	0.0	0.0
Lowest Observed Water Level (31/12/1986)	-0.49	-1.62
Lowest Astronomical Tide (LAT) (29/9/2019)	-1.91	-6.27
Station Datum	-0.74	-2.44

**Values are shown relative to MLLW, which is referenced to the Station Datum*

3.2 Bathymetry

The most recent bathymetric multibeam survey at Yap Port was conducted from May 5 to May 15, 2023 by Sea Engineering, Inc. and was performed to the standards of the U.S. Army Corps of Engineers Hydrographic Surveying Manual EM-1110-2-1003.

Figure 3-2 and Figure 4-1 show the bathymetric contours around the Yap Port and the channel, respectively. Elevation values are referenced to MLLW vertical datum. The depth of the entrance channel ranges from approximately -180 feet (MLLW) to -120 feet (MLLW). Although the channel has been modified in places for shipping, it is a naturally occurring deep water inlet; therefore, outside of the areas of previous dredging, the channel sides are naturally steep, ending in very shallow reef flats. Further into the Yap harbor near the existing wharf area, the depth decreases to -110 feet (MLLW) to -50 feet (MLLW), with a rapid loss of depth towards the shoreline. There are various rock outcroppings and disparate elevated areas throughout the navigation channel within the harbor, and the bathymetric environment of the project area is primarily composed of rock and coral, which could pose hazardous conditions for navigation.

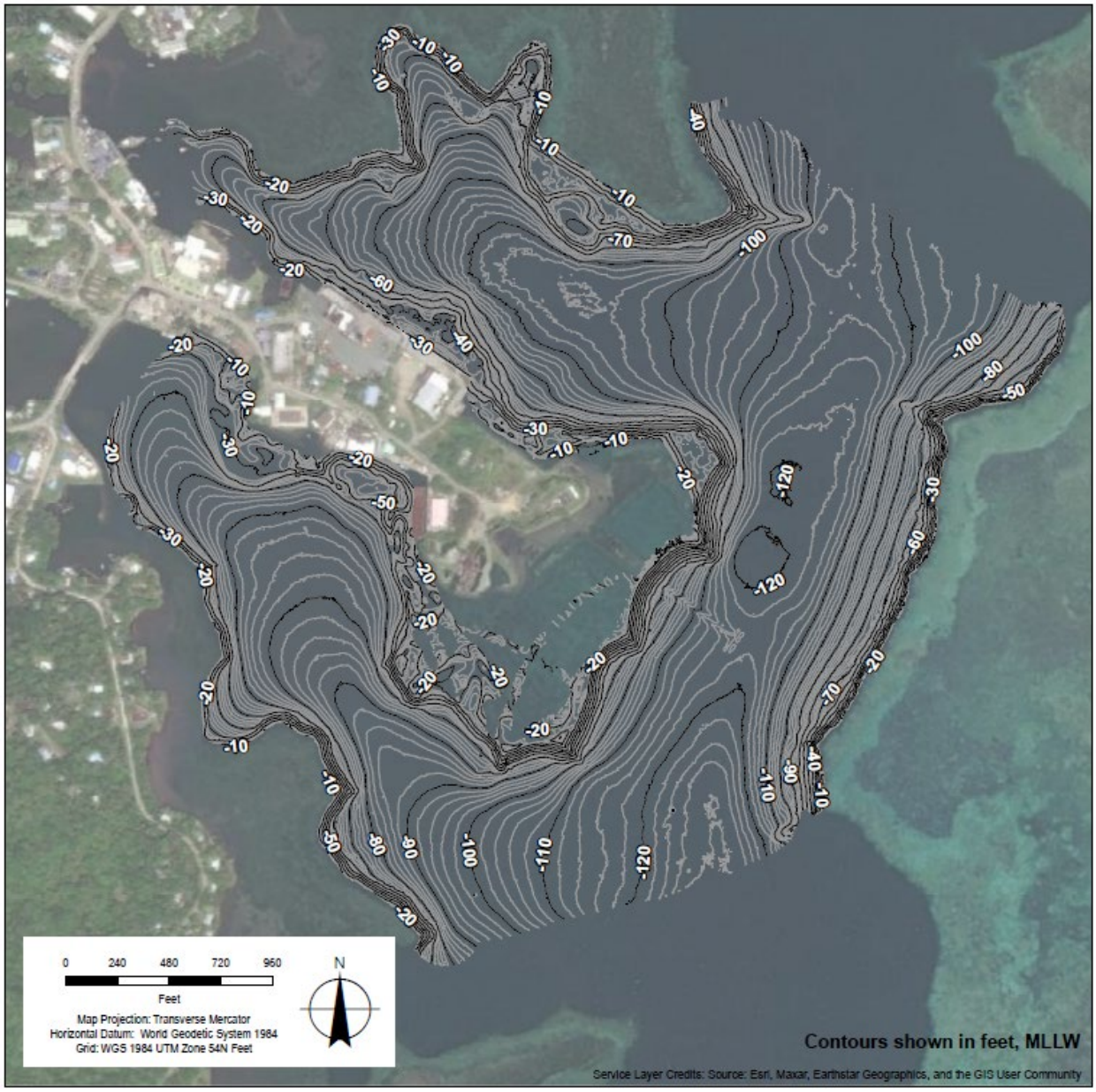

Figure 3-1 Yap Port Bathymetry (Surveyed May 2023 by Sea Engineering, Inc.)

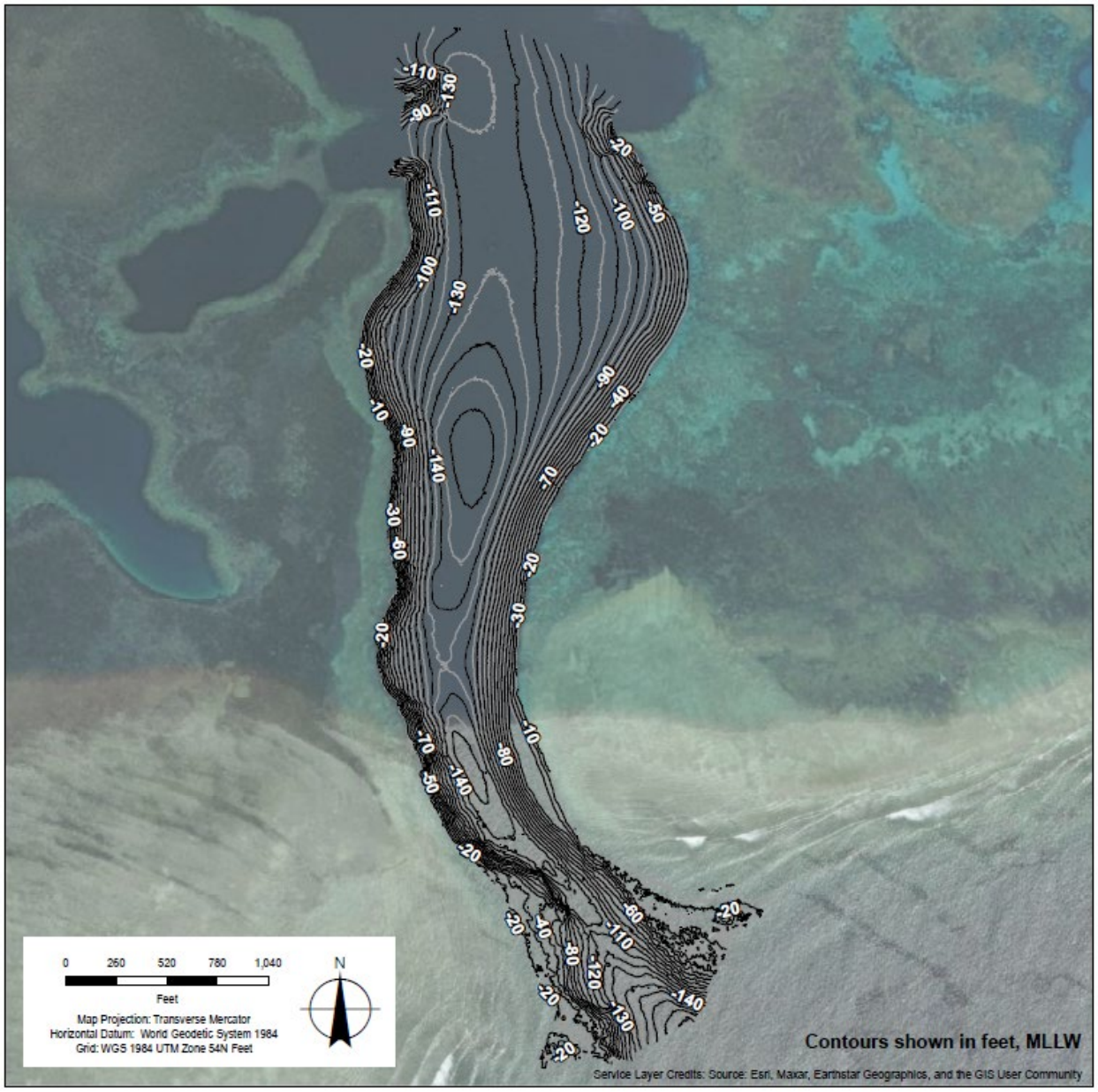

Figure 3-2 Yap Channel Bathymetry (Surveyed May 2023 by Sea Engineering, Inc.)

3.3 Winds

Wind, while blowing over water, applies shear stress to the water surface that generates and promotes the growth of waves. Wind data was sourced from the European Centre for Medium-Range Weather Forecasts (ECMWF) Reanalysis v5 (ERA5), which is a fifth-generation ECMWF atmospheric reanalysis of the global climate generated by the Copernicus Climate Change Service (Hersbach, et al., 2018). The ERA5 model provides hourly estimates of atmospheric and oceanic variables at 0.25° arc degree resolution.

Wind extracted from the ERA5 model is provided at 10 min timesteps at 10 m height above the sea surface. Figure 3-3 displays monthly-averaged wind speed and direction data over a 10-year period spanning 2015 to 2024. Figure 3-4 shows Windrose plots for each month generated from the same data. The wind direction is predominantly north-easterly between November and May, gradually shifting to easterly in June, and

primarily south-westerly between July and October. Wind speeds also tend to be stronger during the north-easterly/easterly-dominated period, with monthly averaged values ranging from 4 m/s to 10 m/s. In contrast, the average wind speed is generally less than 8 m/s from June to August.

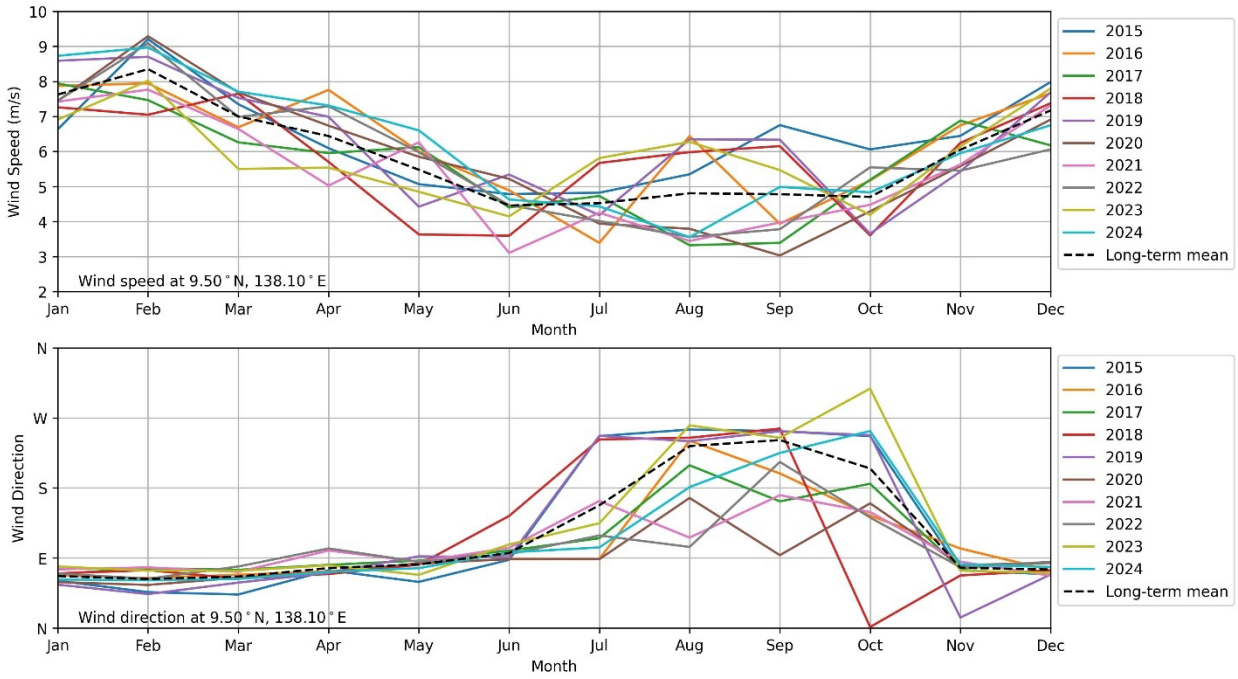

Figure 3-3 Monthly averaged wind speed (top) and wind direction (bottom) during 2015 -2024

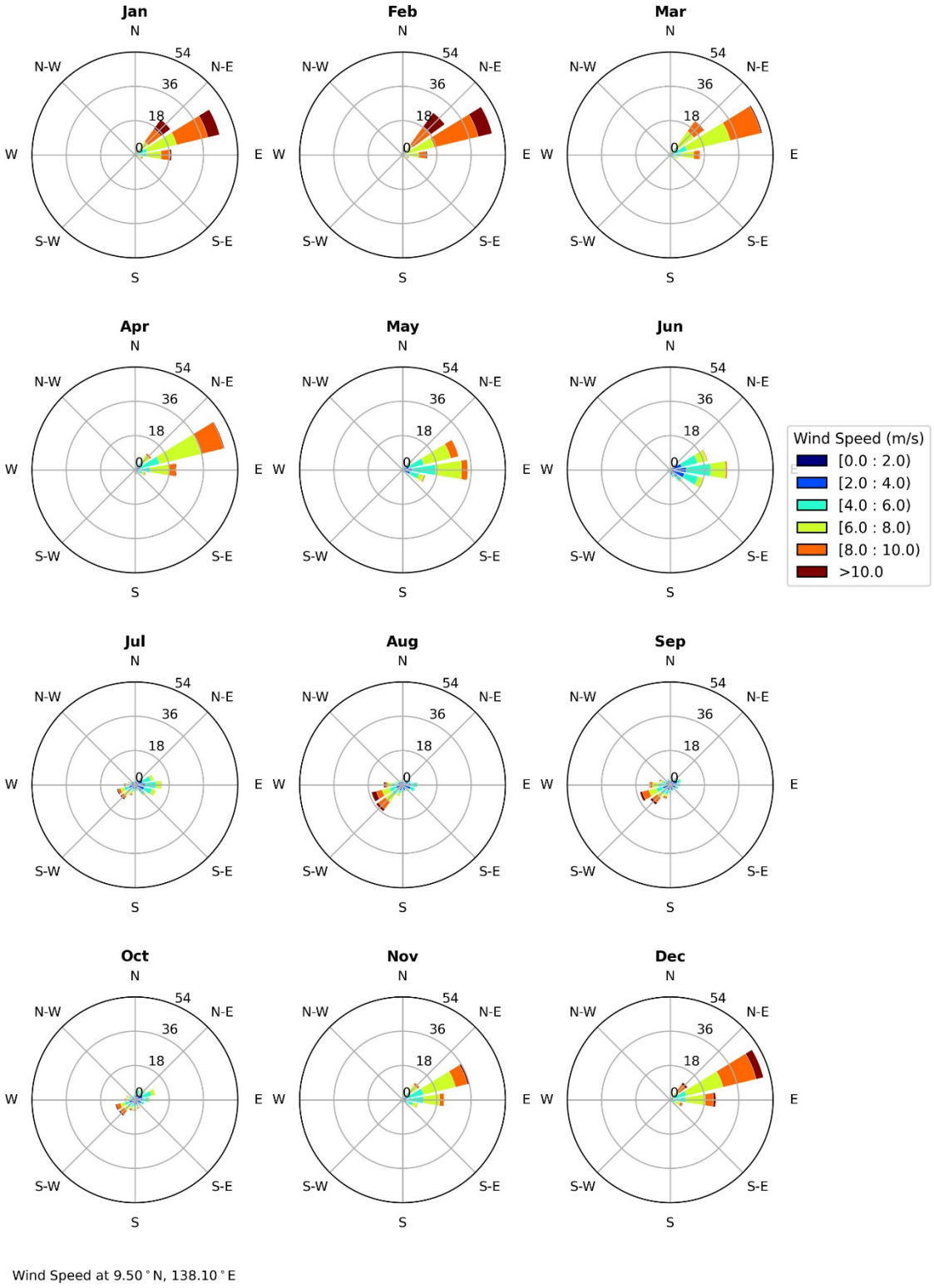

Figure 3-4 Monthly wind roses near the Yap Port based on 2015 to 2024 ERA5[1]

[1] Convention for wind directions is the direction wind is going *from*

3.4 Waves

Offshore wave information (swell and wind waves) near the site was extracted from the CAWCR wave hindcast aggregated collection dataset (Durrant et al., 2019) The CAWCR wave hindcast was performed using the WaveWatch III model utilizing a series of grids with a global grid resolution of 0.4 arc degrees (Durrant et al., 2014), and a refined resolution of up to 4 arc minutes (0.066 arc degrees) within Australia and the Pacific region. The hindcast has been validated by CAWCR using both satellite altimeter observations and available buoy measurements.

Monthly-averaged wave power calculated from extracted CAWCR data between 1993 and 2022 are presented in Figure 3-5. The wave power 10,000 J/s/m in January to an annual minimum of ~3,000 J/s/m in September. Monthly-averaged wave power varied greatly between in the subsequent months, ranging from ~5,000 – 20,000 J/s/m, with a generally increasing trend throughout June to December.

Figure 3-6 presents monthly grouped wave roses summarizing significant wave height and wave direction. Wave direction is predominantly from the east throughout the year. Significant wave heights reach up to approximately 2 m between December and March and are generally around 1 m for the remainder of the year.

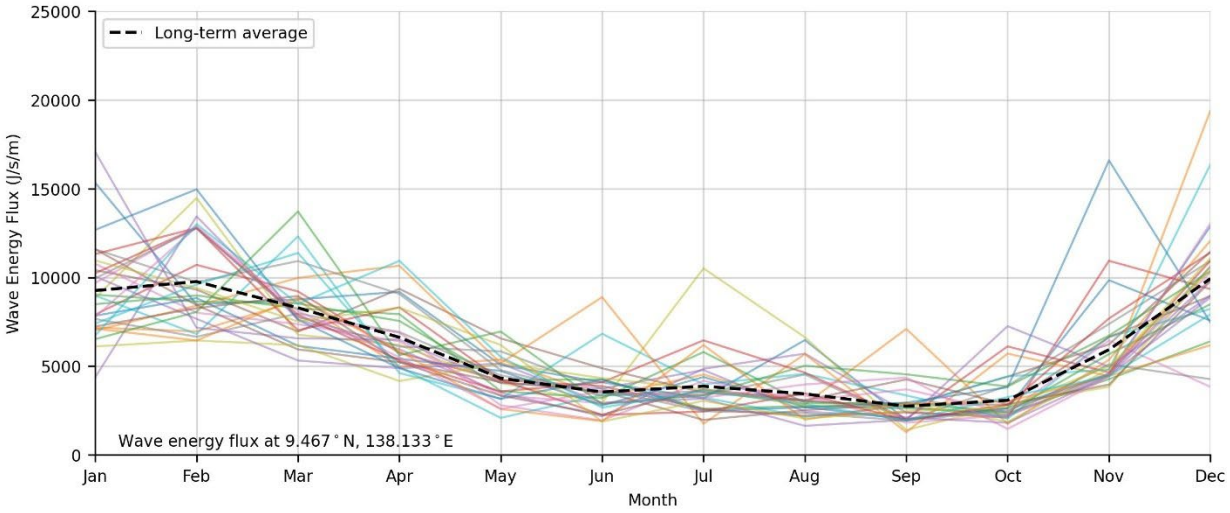

Figure 3-5 Wave power extract from entrance channel offshore covering 30-year period between 1993 and 2022

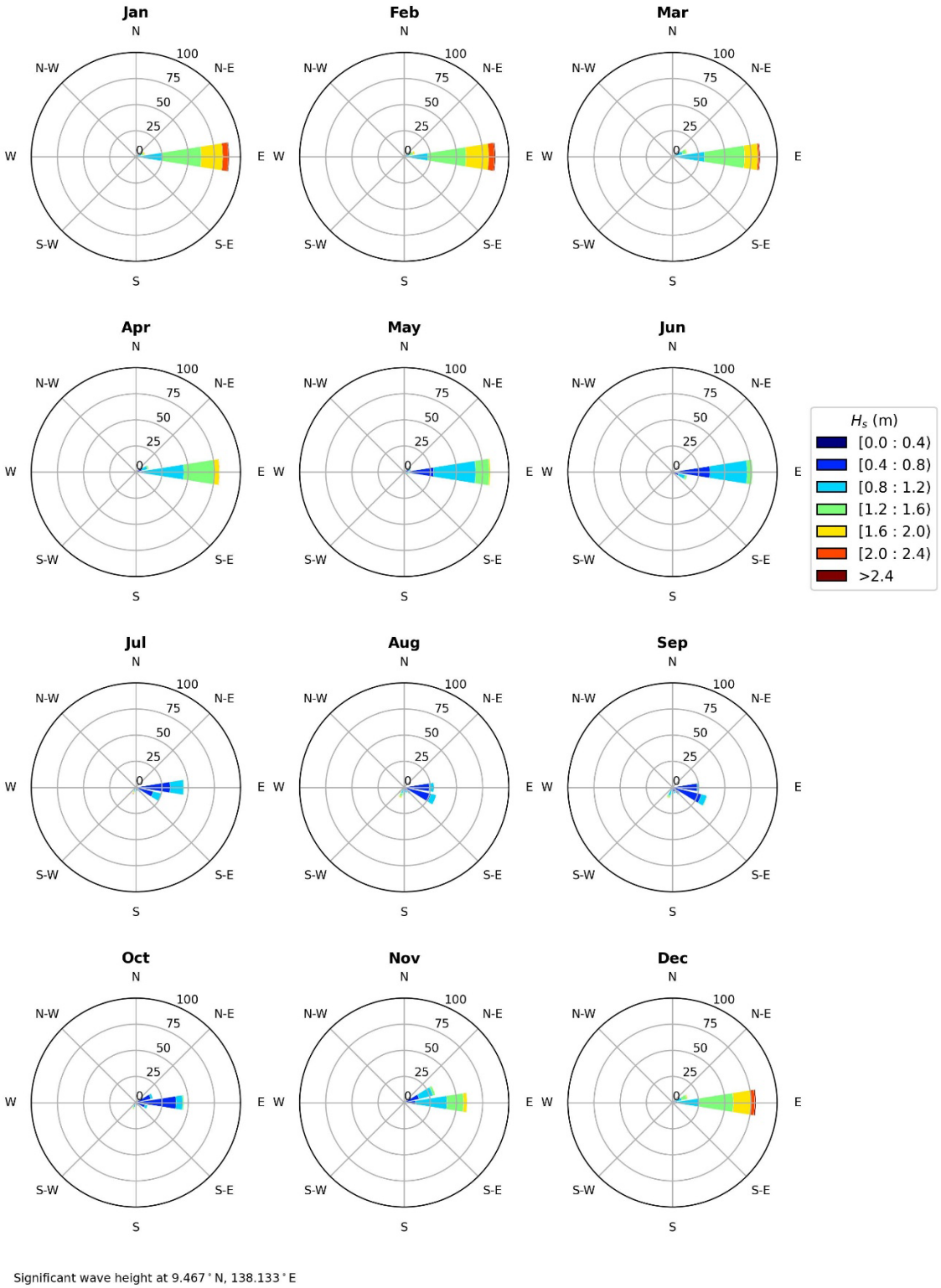

Figure 3-6 Significant wave height rose plot with 30-year wave data between 1993 and 2022[2]

[2] Convention for wave directions is the direction wave is going *from*

4 Metocean Modelling

4.1 Modelling Framework

The dispersion, settling (deposition) and resuspension (erosion) of fine sediments in shallow marine environments is determined by factors such as water levels, tidal flows, waves and oceanographic processes. To simulate these key processes, the following models were developed:

- The DHI MIKE Three-Dimensional (3D) Flexible Mesh (FM) Hydrodynamic (HD) model was used to simulate the 3D hydrodynamics that result from tides, winds, the Coriolis force and air pressure variations. The unstructured FM allows flexibility for tailoring grid resolution in the model domain. This allows optimization of computational performance by providing high resolution in the areas surrounding the Project site and lower resolution elsewhere, where impacts are unlikely.
- The MIKE Spectral Waves (SW) module was used to simulate the wave conditions within the model domain. Wave processes are an important dynamic for sediment dispersion modelling due to the influence of vertical wave circulation on sediment deposition and erosional processes.

The HD and SW models provide the current and wave inputs to the MIKE 3 Mud Transport (MT) model that simulated the dispersion, deposition and erosion (re-suspension) of sediments generated during the dredging and disposal activities.

The modelling framework is conceptualized in Figure 4-1, including the following components:

- Spatially and temporally varying simulated hindcast winds from the ERA5 reanalysis (Hersbach et al., 2020) were applied across the surface of the model domain for the HD model.
- Spatially and temporally varying water levels and current velocity profiles were sourced from the global tide model TPXO 9 (Egbert & Erofeeva, 2002) and the Hybrid Coordinate Ocean Model (HYCOM) (Chassignet et al., 2007) and applied to the offshore boundaries of the MIKE HD model. Spatially and temporally varying temperature and salinity profiles were also sourced from HYCOM and applied at the offshore boundaries.
- Additional spatially and temporally varying meteorological parameters were sourced from ERA5 Reanalysis (Hersbach et al., 2020) as inputs for the heat exchange sub-module within MIKE3 HD, which simulates the transfer of heat between the water surface and the lower atmosphere.

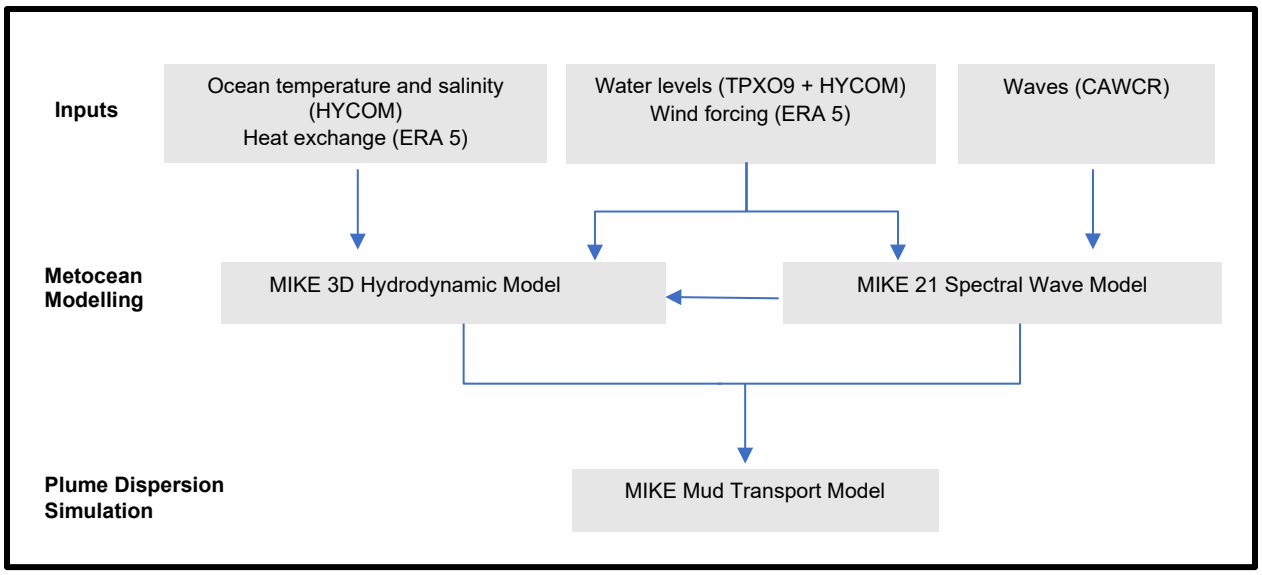

Figure 4-1 Modelling Framework

4.2 Approach

The MIKE 3 FM modelling platform was developed by the Danish Hydraulic Institute (DHI) and is an industry standard for three-dimensional (3D) hydrodynamic modelling. The model domain in MIKE 3 FM is defined horizontally by an irregular network of triangles (the model 'cells') that are split into vertical 'layers' by either a z-level (defined layer thicknesses), sigma coordinate (fixed number of vertical layers throughout the model domain), or a combined sigma and z-level configuration. For each model cell, MIKE 3 FM simulates a range of hydrodynamic properties including, but not limited to, current speed, current direction, water level and salinity. MIKE 3 FM is driven by user-defined environmental inputs (e.g., tidal level variations at open boundaries, wind speeds and directions over the surface, and point-source inputs such as diffusers).

4.2.1 Model Domain

The model domain, mesh triangulation and bathymetry are shown in Figure 4-2 - Figure 4-3. Mesh element sizes ranged from ~6 km (~3.7 mi) at the offshore boundaries (Figure 4-2) to ~25 m (~82 ft) in the vicinity of the Yap Port and the entrance channel (Figure 4-3 and Figure 4-3).

The vertical domain in the 3D model was configured as follows:

- A sigma coordinate system comprising 10 layers in the upper 50 m of the water column, which expand and contract in response to water level variations.
- A fixed coordinate system comprising 16 lower layers (shallow to deep) with thicknesses of two 25 m layers, two 50 m layers, followed by 100 m, 200 m, five 500 m layers, and five 1000 m layers.

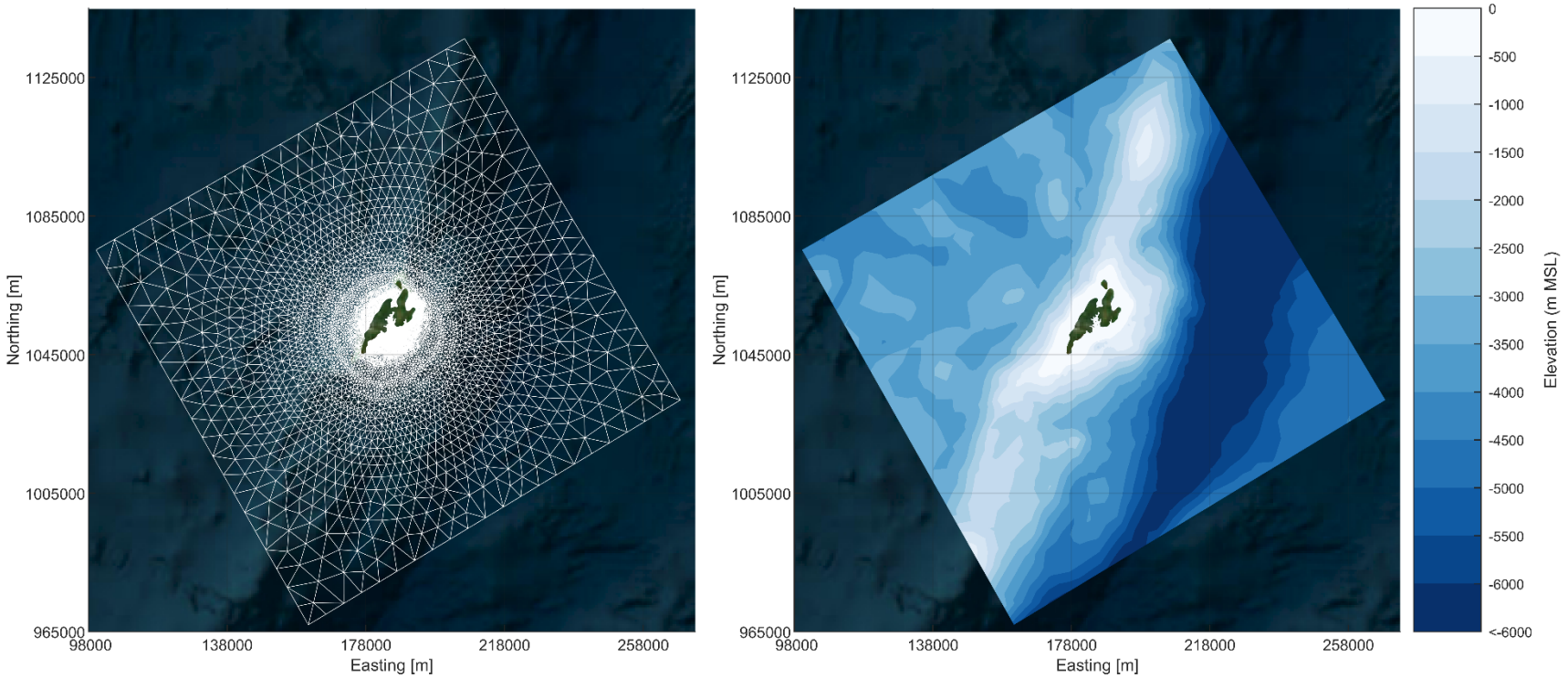

Figure 4-2 ***Model mesh (left) and bathymetry (right) of the entire model domain (datum: MSL)***

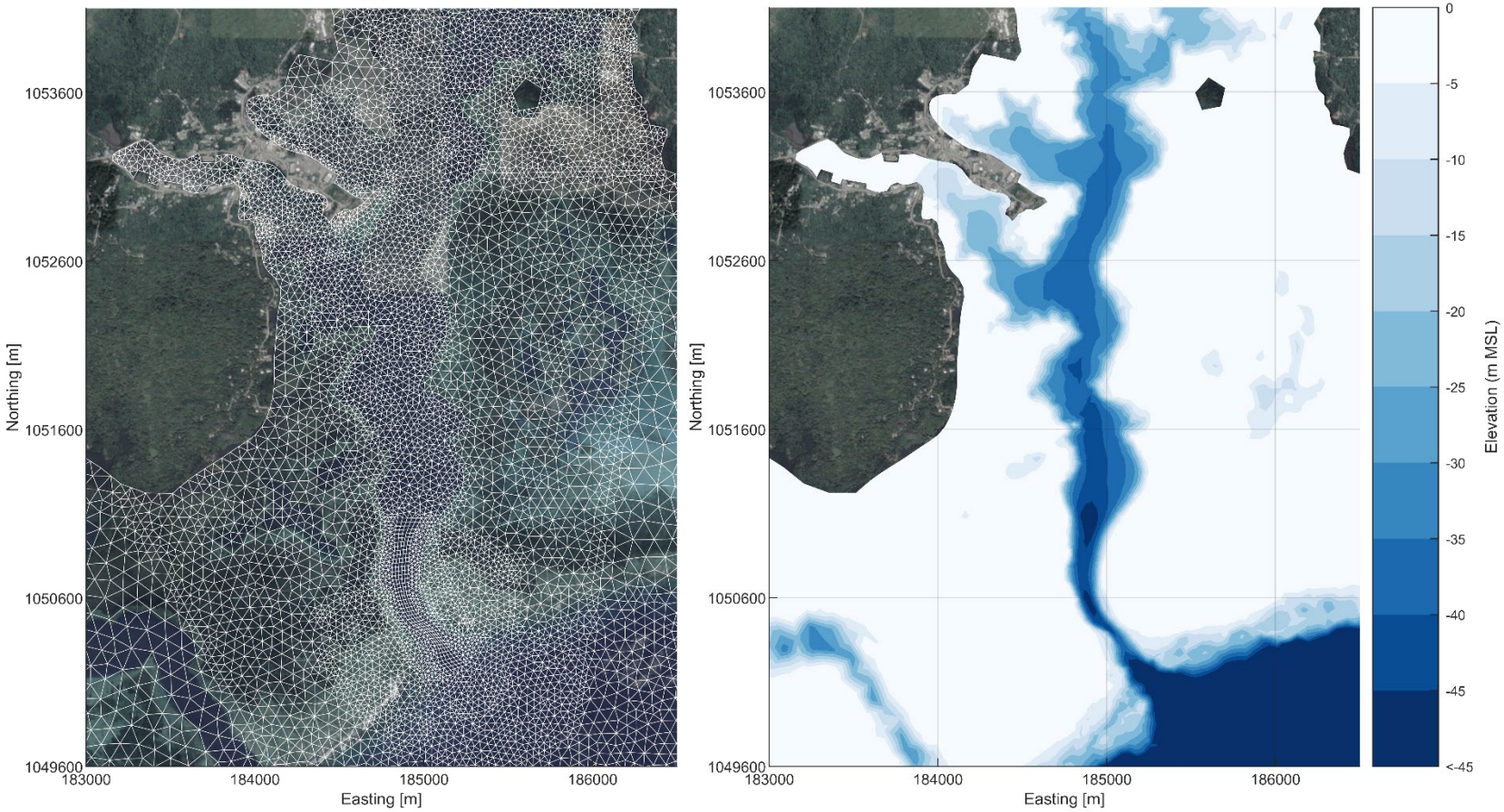

Figure 4-3 Model mesh (left) and bathymetry (right) of the model domain near Yap Port (datum: MSL)

4.2.2Representative Year

To facilitate the simulation of the ambient metocean scenarios, a representative year was selected based on 30-years of wave information from the CAWCR hindcast. The selection criteria for the representative year was based on the annual cumulative wave power. The extraction point selected for the analysis was offshore from Yap Port as illustrated in Figure 4-9.

The results of this analysis indicate that 2011 and 1993 are defined as the low wave year and high wave year, respectively. The annual cumulative wave energy flux for the year 2020 closely matches the long-term average results and aligns well with both the long-term average wave power and significant wave height distributions (). Therefore, 2020 was selected as the representative year.

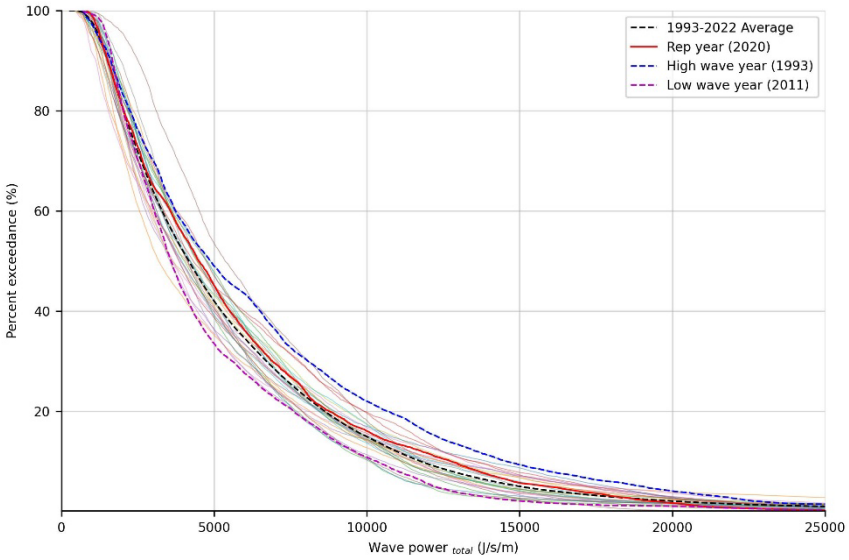

Figure 4-4 Percent exceedance plots for significant wave height (left) and wave energy flux (right)

Within the representative year of 2020, two seasonal periods were selected (based on wind conditions) for simulating the dredging operations. A windy spanning January to February and a calm period spanning July to August were adopted as outlined in .

Table 4-1 Simulation Period

Scenario	Model Ramp-up Periods	Simulation Periods
Windy	25/12/2019 – 01/01/2020	01/01/2020 – 01/03/2020
Calm	24/06/2020 – 01/07/2020	01/07/2020 – 30/08/2020

4.2.3Bathymetry

Due to the large area covered by the model, four different sources of bathymetry data were used.

- GEBCO – A coarse bathymetry dataset retrieved from the General Bathymetric Chart of the Oceans (GEBCO) with a resolution of 15 arc-seconds for the regional model.
- MIKE C-Map – Seabed elevation data from digitized nautical charts.
- EOMAP SDB – Satellite-derived bathymetry (SDB) procured from EOMAP.
- MBES – 2023 multi-beam bathymetric survey performed by Sea Engineering, Inc (Site specific data collected for this project).

The different sources were collated and processed, ensuring that all sources have the same horizontal (UTM Zone 54) and vertical (MLLW) datum. The EOMAP and MBES datasets were utilized as the first priority for defining model depths in the areas covered by the respective datasets, with the coarser resolution C-map and GEBCO data used to supplement the bathymetry in the areas lacking EOMAP or MBES data. Figure 4-5 and Figure 4-6 illustrate the extent of the bathymetric data.

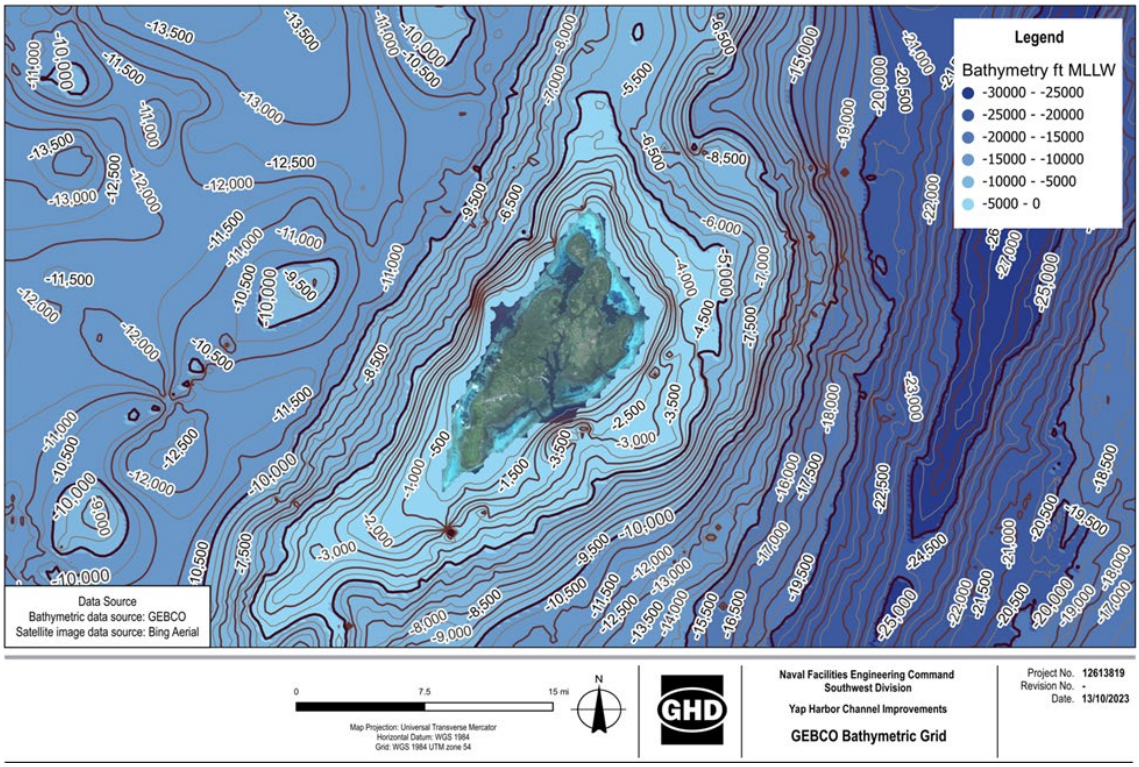

Figure 4-5 Offshore Bathymetry of Yap Island, Excerpt from GEBCO (horizontal datum: WGS 84 / UTM Zone 54, vertical datum: ft MLLW)

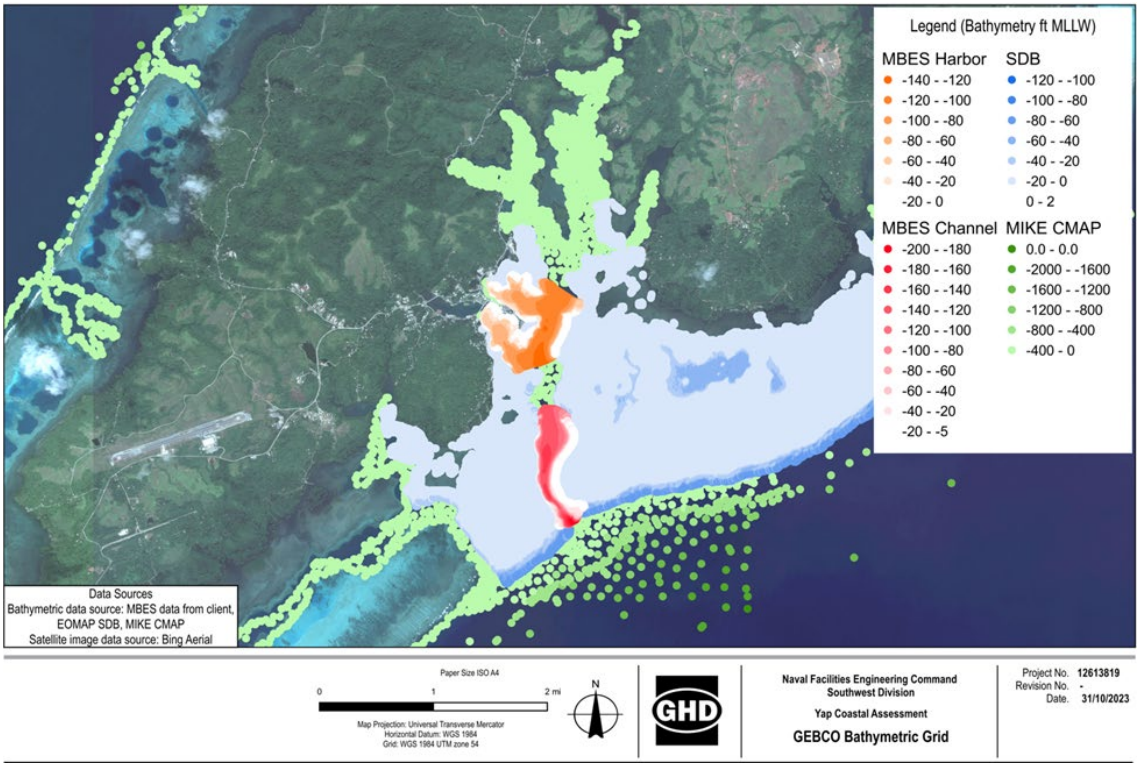

Figure 4-6 ***Additional Bathymetric Data Sources Closer to the Project Site, Consolidated to a Single Horizontal and Vertical Datum (Horizontal datum: WGS 84 / UTM Zone 54, vertical datum: ft MLLW)***

4.2.4 Wind

Wind extracted from the ERA5 model is provided at 10 min timesteps at 10 m height above the sea surface. The seasonal trend of the wind has been detailed in Section 3.3. Figure 4-7 shows the snapshots of the 2D wind field extracted from the ERA5 model representing a windy condition and a calm condition.

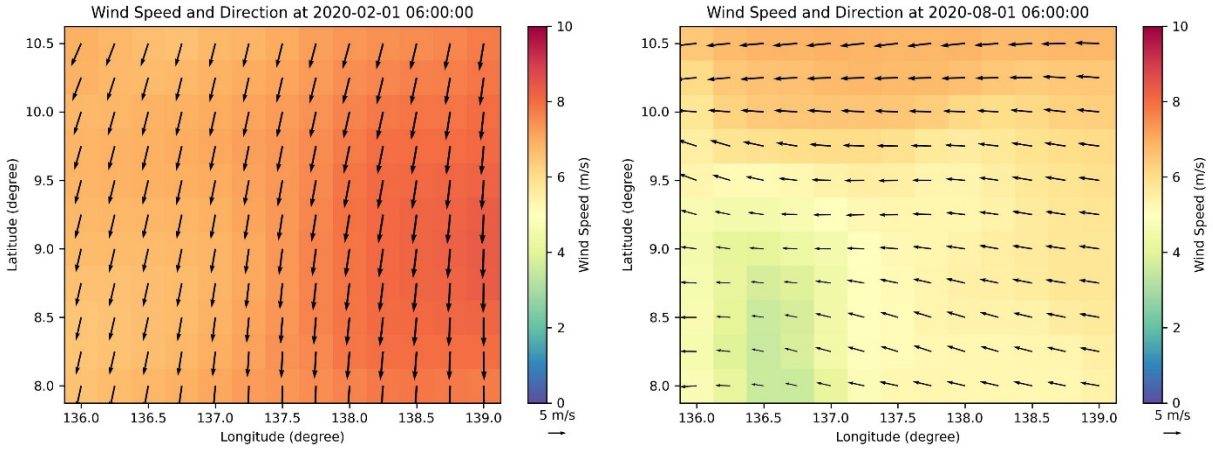

Figure 4-7 ***Snapshots of 2D wind field from ERA5 model with windy condition (left) and calm condition (right)***

4.2.5 Waves

The CAWCR wave hindcast was performed using the WaveWatch III model. The resolution of the CAWCR model around Yap port is 4 arc minutes (0.066 arc degrees). Snapshots of the 2D wave field extracted from CAWCR are shown in Figure 4-8 for energetic and low wave conditions within the representative year of 2020.

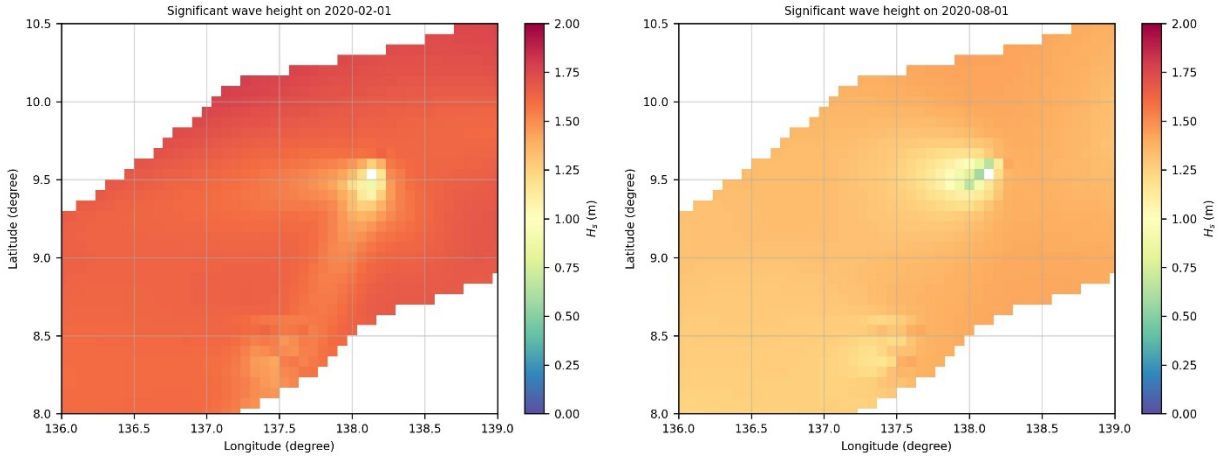

Figure 4-8 ***Snapshots of 2D wave field from CAWCR model with high H_s condition (left) and low H_s condition (right)***

4.3 Model validation

4.3.1Metrics

Model validation was assessed with quantitative indices summarized in Table 4-2. The validation compares the simulated results from the numerical models with the available actual measured data at the site.

Table 4-2 Metrics for evaluating model performance

Metric	Equations
Mean Absolute Error (MAE). A quantitative measure of the absolute differences between the simulation and measurements. Low values of MAE represent good model performance. This metric is easily interpretable and a more natural measure than the commonly used root-mean-squared error, as it is less influenced by extreme values (i.e. outliers or 'noise' in the measured data) (Willmott, 1982).	$$\boldsymbol{MAE} = \frac{\sum_{i=1}^{n}\lvert P_i - O_i\rvert}{n}$$ where: P_i = Predicted value at comparison time i O_i = Observed value at comparison time i n= Number of comparison measurements
Index of Agreement (IOA). IOA is a quantitative measure of the average differences between predicted and observed values relative to the range of values in the observation data (Willmott, 1982). It is bounded between the values of 0 and 1, with values close to 0 describing large relative differences (i.e. poor validation) and values close to 1 describing small relative differences (i.e. good validation). Willmott et al. (1985) suggests that IOA values meaningfully greater than 0.5 represent good model validation, with values approaching 1 representing excellent validation.	$$\boldsymbol{IOA} = 1 - \frac{\sum_{i=1}^{n}(P_i - O_i)^2}{\sum_{i=1}^{n}(\lvert P_i - \bar{O}\rvert + \lvert O_i - \bar{O}\rvert)^2}$$ where: $\bar{O}$ = Mean of the observations during the comparison period.

4.3.2Model validation results

Model validation was performed in comparison to measured water levels, currents, and wave heights. Figure 4-9 shows the measurement locations for water levels, currents and waves. The period of model validation at different sites varied due to the availability of measurement data, as summarized in Table 4-3.

Table 4-3 Model validation variables and period

Site Location	Validating variables	Measurement period
Yap port	Water level	29/08/2024 – 31/10/2024
Entrance Channel	Current, Wave	29/08/2024 – 31/10/2024
Turning Basin	Current, Wave	29/08/2024 – 31/10/2024

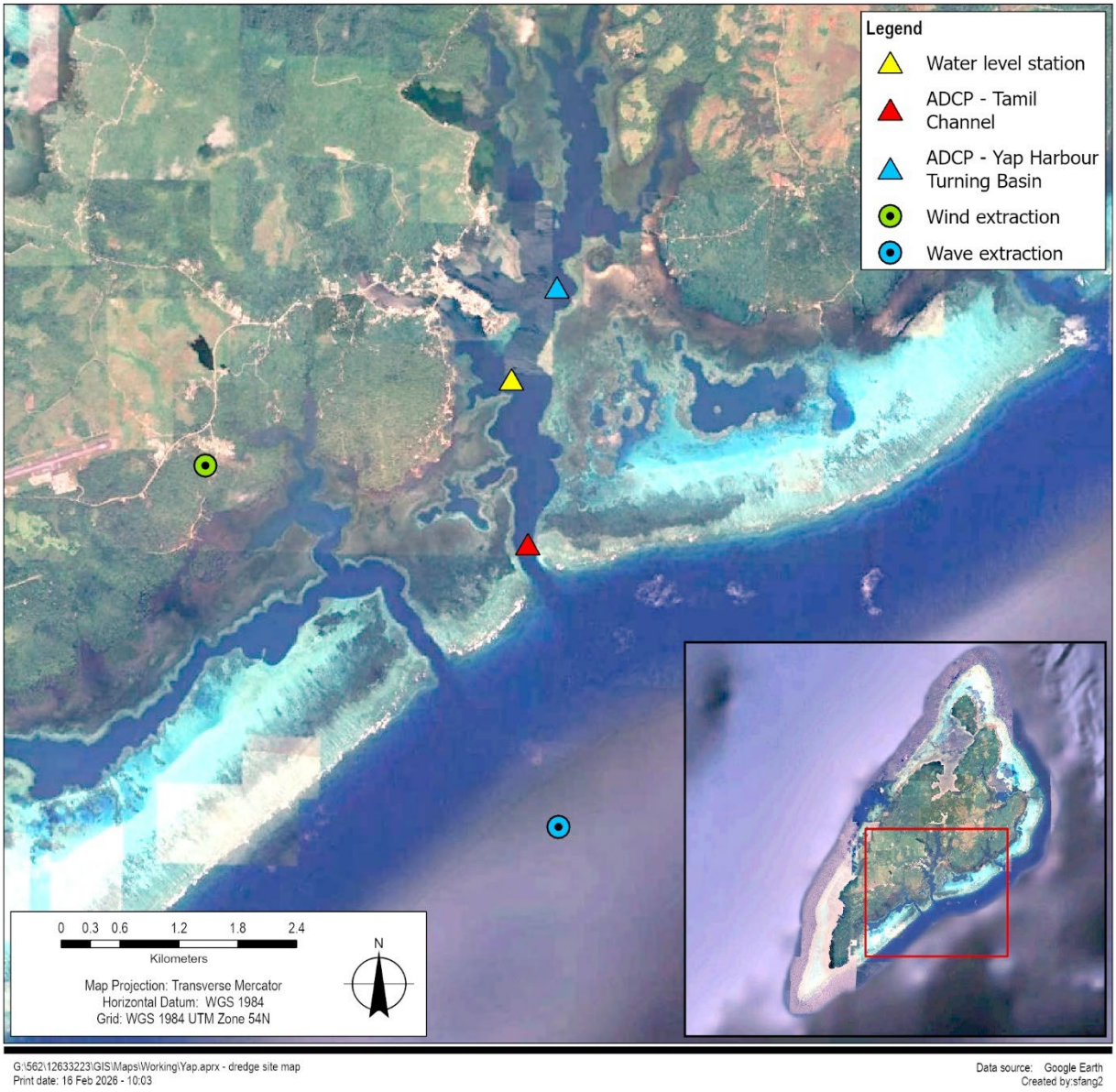

Figure 4-9 Location of the site measurements and data extraction

The validation results of both hydrodynamic modelling and spectral wave modelling demonstrated agreement between the measured and simulated data, thereby providing confidence in the model's ability to accurately simulate the metocean conditions of the Project site.

A reasonable agreement was achieved for comparisons of the spectral wave model predictions to the measured significant wave height with IOA of 0.83 and MAE of 0.05 through the entrance channel, and IOA of 0.54 and MAE of 0.04 at the proposed turning basin.

For the peak wave period, qualitative agreement was observed between the time series comparisons at the entrance channel, although less agreement was observed during low wave periods, corresponding to significant wave heights less than 0.3 m. At the turning basin, measured significant wave heights were consistently low (generally < 0.2 m) due to the sheltering effect of the fringing reef system. Under very calm

conditions, the algorithms used to process wave measurements and estimate wave periods often do not return a clear signal. Several short-duration events were identified in the turning basin dataset during which the measured peak wave period shifted from a sea-dominated regime (< 5 s) to a swell-dominated regime (> 8 s). These events were often not replicated by the model; however, they occurred during periods of very low wave heights (< 0.1 m), when wave energy at both sites was minimal regardless of wave period. Conversely, the model occasionally predicted swell-dominated conditions during periods of very low wave height when the measurements indicated sea-dominated conditions. This will be considered in the assessment of the results of the plume modeling.

Minor divergence between the model and the site-specific measurements during these periods do not represent significant discrepancies in wave energy; however, they can result in numerical differences that reduce the IOA and increase the MAE. The model's strong performance in reproducing measured significant wave heights, together with agreement in peak wave period during larger wave events, provides confidence that the model reasonably represents the wave energy of the system and is suitable for its intended purpose.

The verification assessment confirms that the hydrodynamic and spectral wave models are well-suited for evaluating the sediment plume dispersion at Yap Port. The agreement between measured and simulated data enhances confidence in the model's ability to accurately reproduce the dispersive forces important for determining potential impacts from dredging operations.

Table 4-4 Summary of model verification results for hydrodynamic modelling

Site Location	Vertical Location	Validating Variables	Unit	IOA	MAE
Yap port	Surface	Water level	m	0.99	0.07
Entrance Channel	Surface	U (east-west) Velocity	m/s	0.70	0.02
		V (north-south) Velocity	m/s	0.87	0.06
		Current Speed	m/s	0.70	0.05
	Mid-depth	U (east-west) Velocity	m/s	0.79	0.02
		V (north-south) Velocity	m/s	0.89	0.06
		Current Speed	m/s	0.76	0.06
	Bottom	U (east-west) Velocity	m/s	0.72	0.03
		V (north-south) Velocity	m/s	0.81	0.09
		Current Speed	m/s	0.69	0.07
Turning Basin	Surface	U (east-west) Velocity	m/s	0.38	0.02
		V (north-south) Velocity	m/s	0.59	0.02
		Current Speed	m/s	0.48	0.02
	Mid-depth	U (east-west) Velocity	m/s	0.41	0.02
		V (north-south) Velocity	m/s	0.50	0.02
		Current Speed	m/s	0.41	0.02
	Bottom	U (east-west) Velocity	m/s	0.34	0.02
		V (north-south) Velocity	m/s	0.44	0.02
		Current Speed	m/s	0.32	0.02

Table 4-5 Summary of model verification results for spectral wave modelling

Site Location	Validating Variables	Unit	IOA	MAE
Entrance Channel	Significant wave height	m	0.83	0.05
	Peak wave period	s	0.41	2.08
Turning Basin	Significant wave height	m	0.54	0.04
	Peak wave period	s	0.49	4.01

5 Plume dispersion modelling

5.1 Model set-up

The plume dispersion modelling was carried out using the MIKE Mud Transport (MT) module, developed by DHI. This model is well-suited for simulating the transport and fate of fine sediments (silt and clay-sized particles) in coastal and estuarine environments, where dredging, reclamation, or sediment resuspension activities may affect water quality or sensitive habitats.

The MT module was driven by a decoupled hydrodynamic model, developed for a representative year, and was further coupled with the spectral wave field output from the wave model. The hydrodynamic model provides the water level, velocity and current-induced bed shear stress fields, while the wave model supplies the wave-induced bed shear stresses and vertical circulation dynamics, both of which are key drivers of sediment transport and plume dispersion.

Given that the project site is subject to seasonal variability in met-ocean conditions, particularly in wind and wave regimes, the dredging activity was simulated over two seasonally-varying periods of high and low wind conditions within the representative year as outlined in Section 1.1.This seasonal differentiation enables a more robust assessment of plume dispersion under a range of environmental forcing scenarios. Table 5-1 summarizes the MT simulation period, which included 28 days (4 weeks) following completion of the dredging activity to allow for continued simulation of the dispersion and deposition of sediments remaining in suspension at the end of dredging.

Table 5-1 MT simulation summary

Scenario	Model ramp-up periods	Dredging start date	Dredging end date	Simulation end date
Windy	25/12/2019 – 01/01/2020	01/01/2020	01/02/2020	01/03/2020
Calm	24/06/2020 – 01/07/2020	01/07/2020	01/08/2020	30/08/2020

5.2 Dredging specifications

5.2.1 Sediment composition

Composite sediment samples collected from near-surface layers at the proposed dredging sites, were sourced from GEOLABS (2025). These site-specific samples were used to determine the fines content in the sediment to be modeled. The sampling indicated that 12% of the marine sediments within the dredging areas are comprised of fines.

5.2.2 Sediment settling velocities

Sediment settling velocities adopted in the modelling are summarized in Table 5-2, which have been calculated using empirical relationships from Cheng (1997). The model simulated the fine particles (clay and silt-sized fractions) exclusively to predict far-field SSC and deposition. Larger particles settle rapidly out of suspension and deposit on the seabed in close proximity (typically tens of meters) to the dredger/disposal site. These are not modelled as they are incorporated into the volume of material 'dredged' from the footprint. Five distinct fines fractions for clay and silt-sized particles were defined for the modelling on the basis of the sampling data outlined in Section 5.2.1. The composition of clay and silt particles in the model was evenly distributed between the Wentworth grain classes for clay (one class) and silt (four sub-classes) at 20% each.

Table 5-2 Summary of simulated fine particle distribution and settling velocities

Wentworth Grain Classification	Bin mid (mm)	Percentage of total fines (by volume)	Settling Velocity (mm/s)
Clay (0-4 µm)	0.002	20.0%	0.00235
Very Fine Silt (4-8 µm)	0.006	20.0%	0.0211
Fine Silt (8-16 µm)	0.012	20.0%	0.0843
Medium Silt (16-32 µm)	0.0235	20.0%	0.322
Coarse Silt (32-62.5 µm)	0.0465	20.0%	1.24

5.2.3 Sediment source terms

The derivation of fine sediment fluxes ("sediment source terms") for this study followed the methodology of Becker *et al.* (2015). The calculation steps and reference sources are outlined in Table 5-3 for the constituent dredging areas and summarized as follows:

- A large backhoe dredger (BHD) will be utilized, with an average production rate of 200 m^3/hr of *in-situ* dredged material.
- Based on the total volume of dredged material and the dredging rate, the duration of the dredging operations was calculated as 31.6 days, considering daily operational availability of 70% (16.8 operational hours per day) and an operational schedule of 6.5 days per week (allowing a 12-hour shut-down on Sundays).

- Losses due from the BHD bucket during dredging (termed 'bucket drip') were estimated based on the bucket drip fraction (far-field source term for percentage of fines generated that contribute to the far-field plume) published ranges available in Becker *et al.* (2015). For placement at the disposal sites (the reclamation sites are adjacent to the disposal sites at Rull and Tamil,) the published range for BHD bucket drip fraction is between 1% and 4%. 4% was conservatively adopted as an upper-range value of the proportion of fines that contribute to a far-field plume generated by a BHD operating at the seabed of the disposal site. This assumption was used for all locations and sediment types.

The adopted source term for the BHD is **0.37 kg/s**.

The outflow of the fine sediment from the disposal sites (Tamil, Rull and Nungoch) were considered as another sediment source term in the MT simulations. For the purposes of being conservative, the mechanically excavated material is assumed to be barged or trucked to the disposal site and then deposited directly onto the seabed. The coarser material is allowed to settle and consolidate within the disposal footprint, while the excess water, which may still contain suspended fine sediment particles, will flow back into the harbor. It is assumed that disposed sediments at each disposal site will first be used to construct bunds along the boundary of the disposal footprint. Subsequent disposal of sediments will be between the bunds and the existing shoreline. This is likely not representative of what will occur at all three disposal sites, since much of the deposited material will be above the water line. However, for the purposes of this simulation, the most onerous case is adopted.

The calculations for determining the disposal source term at each disposal are presented in Table 5-4, and summarized as follows:

- All particles larger than fines are assumed to deposit within the disposal site.
- Assuming the disposal impact is continuous, even though the dredging activities have a 70% daily efficiency and a 6.5-day per week schedule, the impact of disposing materials into the marine environment will be continuous rather than intermittent, starting after the first disposal (conservative assumption).
- The liquid flow rate out of the disposal/reclamation site is assumed to be the same as the incoming flow rate i.e. there are no liquid losses to infiltration or evaporation (conservative assumption).
- For the volume disposed of at three disposal sites, the model simulated the fill only up to high tide (3.63 ft above MLLW), with a maximum theoretical volume of reclamation material that could release total fines of 14,144 m^3.
- Assuming that the settlement of fine particles within the bunds of the disposal site (in-hopper settlement) is 75%, the disposal outflow fines flux discharged to the marine environment at stockpile sites is calculated as **0.10 kg/s.**
- On the basis of the conservative assumptions adopted as outlined above, the dredge scenarios simulated in this study are considered a **worst-case scenario**.

Table 5-3 ***Mass flux estimates for all sites across Yap Port dredging***

Item	Value	Unit	Source
Sediment characteristics			
Total in situ volume	99,426	m^3	GHD COWI (2025a)
Dry density	1,378	kg/m^3	Calculation
Fines percentage	12.0	%	GEOLABS (2025)
Dredge details			
In situ production (hourly)	200	m^3/hr	GHD COWI (2025a)
Operational schedule	24	hr	GHD COWI (2025a)
	6.5	days /week	GHD COWI (2025a)
Operational availability	70	%	GHD COWI (2025a)
Dredging duration (cumulative active dredge time)	497.1	hrs	Calculation
Total days of dredging at 70% availability	29.6	days	Calculation
Total dredge program duration at 6.5 days per week	31.6	days	Calculation
Key Model details			
Total amount of fines	16,436,125	kg	Calculation
In situ production rate	0.06	m^3/s	Calculation
BHD details			
BHD bucket drip fraction	4	%	Becker *et al.* (2015)
Fines to far-field	657,445	kg	Calculation
Model source terms			
Flux bucket drip	**0.37**	**kg/s**	Calculation

Table 5-4 Calculation of sediment flux from disposal outflow at disposal/reclamation sites

Item	Value	Unit	Remark
Volume into the reclamation site	14,144	m^3	The volume equivalent to the filled material up to high tide.
Fines production	9.18	kg/s	Calculated from the total in situ dredge mass applied with the fines fraction and dived by the total duration.
Fines to reclamation during active dredging	8.82	kg/s	Calculated from the fines production after subtracting the bucket drip flux.
Average rate of fines to disposal over whole dredge program	0.82	kg/s	Average rate considering the 70% of daily operational efficiency of BHD and a weekly schedule of 6.5 working days.
Disposal site settlement factor	75%	%	The factor refers to the settlement of fine particles within the bunds of the disposal site. The reasonable range for in-hopper settlement is 0-100% as stated in Becker *et al* (2015). Larger size of disposal site compared to typical hopper storage would result in longer retention times and higher settling. Adopting 75% settling.
In-matrix fixation	5%	%	The in-matrix fixation represents the entrapment of fines within the matrix of dredged sediments that are deposited at the onshore disposal site. The upper end of range (1-5%) from Becker et al (2015) is considered reasonable due to the mechanical dredging method which retains the natural sediment structure better than hydraulic dredging methods, minimizing disruption of the sediment matrix and allow greater in-matrix fixation.
Fines outflow fraction	15%	%	The fines outflow fraction refers to the fraction of fines in the outflow from the disposal site that contribute to a far-field plume. Applied a conservatively high value that is 75% of the reasonable range (0-20%) from Becker et al (2015) for hopper overflow. Upper end not considered appropriate due to the low energy nature of the outflow compared to hopper overflow, which will encourage greater deposition of fines in the near-field surrounding the reclamation site.
Disposal outflow fines flux	**0.10**	**kg/s**	Fines dispersed to a far-field plume from the reclamation site.

5.2.4 Spatial and Temporal Configuration of Operations

Two dredging scenarios were modelled over different seasons. For each scenario, dredging and disposal activities were configured using a staged approach to hydrodynamic and sediment dispersion modelling to reflect the influence of the changing bathymetry on hydrodynamics as the dredging progresses. For each scenario, the first half of the dredging operation was simulated with the baseline model mesh, while the last half (along with an additional 28 days post-dredging simulation time) adopted the operational-phase mesh, which includes the updated depths at the dredging sites and dredge pocket at disposal sites of Rull and

Tamil, and the reclamation footprint of each disposal site. In this manner, the effect of the dredging activity itself on the hydrodynamics at the site is incorporated into the predictions.

For each scenario, an additional 28 days following the completion of the dredging campaign were simulated in order to track subsequent dispersion and settling of suspended solids remaining within the marine environment. The stage scheduling and details of sediment source terms are described in Table 5-5 and Table 5-6 and for dredging and disposal activities, respectively. The spatial distribution of dredging and disposal locations are illustrated in Figure 5-1 and Figure 5-2.

Note that the water outflow locations for each disposal site were situated near the land boundary, reflecting that outflow always occurred from the edge of the stockpile disposal site. The differences between the part 1 and part 2 disposal locations (Figure 5-2) reflect changes to the dispoal site, where some water cells in the part 1 baseline mesh become land cells in the part 2 operational mesh. Despite these positional differences, the physical meaning of the disposal locations for both part 1 and part 2 remains the same at each disposal site.

Table 5-5 MT model temporal configuration with dredging flux

Dredging Area	Dredge Volume (m^3)	Active Dredge Hours	Dredge Days[3]	Simulation Timing		Number of BHD source points	Flux Per BHD Point (kg/s)
				Windy scenario	Calm scenario		
Berth	18,898	9.49	0.56	01/01/2020 – 01/02/2020	01/07/2020 – 01/07/2020	1	0.37
Turning Basin	19,499	97.50	6.37	01/01/2020 – 07/01/2020	01/07/2020 – 07/07/2020	4	
Rull pocket dredge	11,010	55.05	10.14	07/01/2020 – 11/01/2020	07/07/2020 – 11/07/2020	2	
Entrance Channel West	18,291	91.46	16.09	11/01/2020 – 17/01/2020	11/07/2020 – 17/07/2020	5	
Tamil pocket dredge	7,646	38.23	18.36	17/01/2020 – 19/01/2020	17/07/2020 – 19/07/2020	1	
Entrance Channel East	41,082	205.41	31.59	19/01/2020 – 01/02/2020	19/07/2020 – 01/08/2020	8	
Post - dredging stage	0	0	28	01/02/2020 – 01/03/2020	01/08/2020 – 30/08/2020	0	0

[3] Refers to calendar days

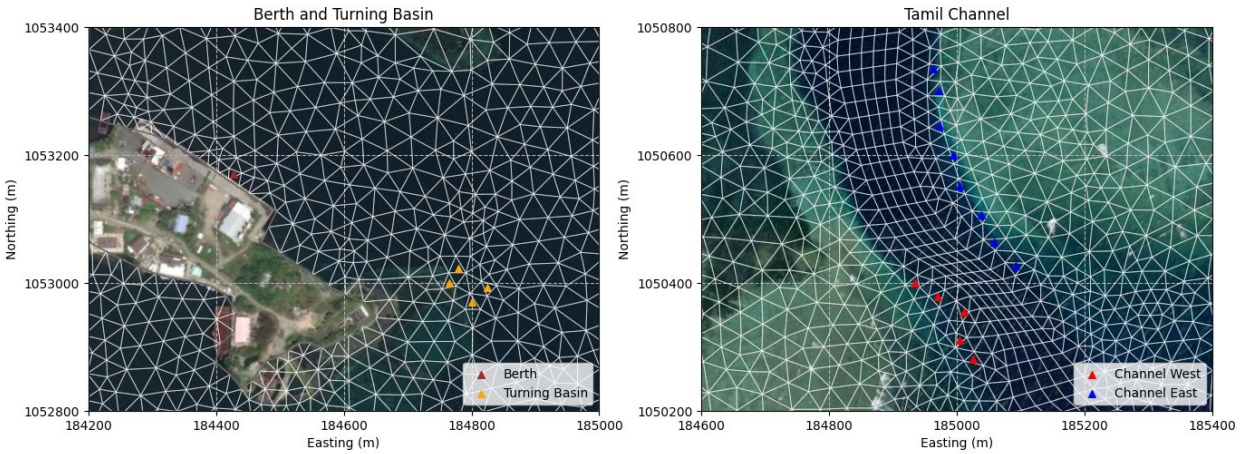

Figure 5-1 Spatial distribution of the dredge site locations

Table 5-6 MT model temporal configuration with disposal fluxes

Disposal Site	Simulation Timing		Number of BHD source points	Flux Per BHD Point (kg/s)
	Windy scenario	Calm scenario		
Nungoch	01/01/2020 – 07/01/2020	01/07/2020 – 07/07/2020	2	0.10
Rull	07/01/2020 – 17/01/2020	07/07/2020 – 17/07/2020	2	
Tamil	17/01/2020 – 02/02/2020	17/07/2020 – 02/08/2020	2	
Cessation of Disposal	02/02/2020 – 01/03/2019	02/08/2020 – 30/08/2019	0	0

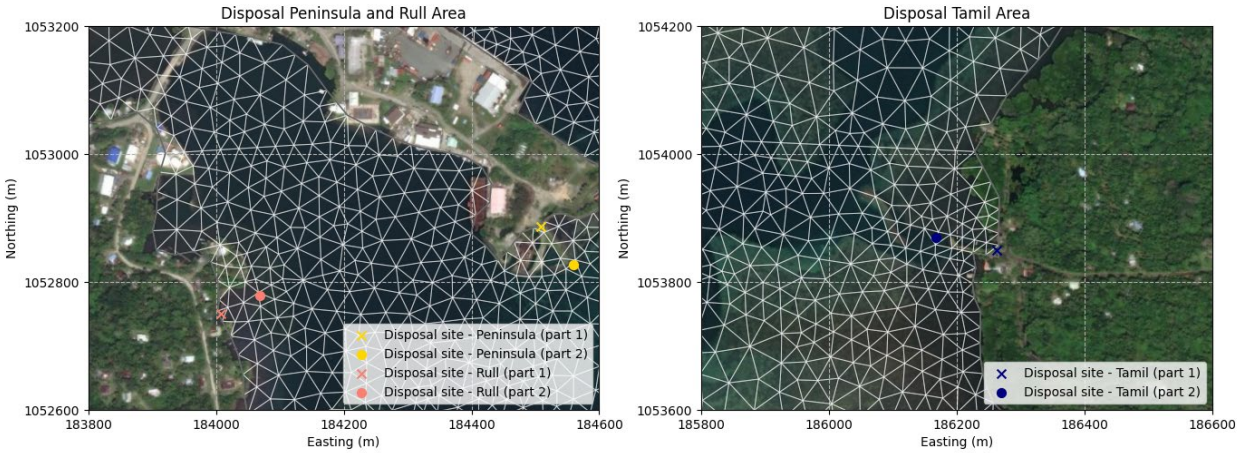

Figure 5-2 Spatial distribution of the disposal site locations

6 Results and discussion

6.1 Suspended Sediment Concentration (SSC)

6.1.1SSC changes

Statistical contours of dredging-induced SSC changes (ΔSSC) were produced for the windy and calm scenarios to demonstrate the extent and relative frequency (via different percentile plots) of SSC increases in the marine environment.

The following plots are presented in Figure 6-1 - Figure 6-8:

- The mean ΔSSC (the numerical average of all simulated concentrations) for both scenarios.
- 75th percentile ΔSSC (corresponding to ~15-days of cumulative exceedance duration over the 60 days simulation) for both scenarios.
- 95th percentile ΔSSC (corresponding to ~3-days of cumulative exceedance duration over the 60 days simulation) for both scenarios.
- The maximum (100th percentile) ΔSSC (corresponding to the instantaneous maximum value at each location that occurred at any time during the simulation) for both scenarios.

The outputs are not depth-averaged; the maximum concentration experience is presented.

For **calm period** simulation (July to August 2020), the model predicted the following:

- The **mean** distance ΔSSC exceeded 50 mg/L extended 75 m from the turning basin dredge site, while ΔSSC remained below 5 mg/L at the other dredging sites. At the disposal sites, the mean distance ΔSSC exceeded 5 mg/L extended up to 250 m, with the highest localized average concentrations predicted to exceed 100 mg/L at Rull (for a very short amount of time) (Figure 6-1).
- ΔSSC exceeding 5 mg/L was predicted to extend 300 m from the edge of the dredging for 5% of the time (corresponding to the 95th percentile plots in Figure 6-3). The spatial extents of sediment plumes from the disposal sites were generally larger, extending 120 m and 800 m from the edge of the disposal sites for 25% and 5% of the time (Figure 6-2 and Figure 6-3).
- Dredging activities were predicted to generate ΔSSC of less than 50 mg/L for more 95% of the time (Figure 6-3). Disposal activities resulted in predicted ΔSSC exceeding 50 mg/L at distances of up to 150 m from the Rull for 5% of the time.
- The maximum ΔSSC exceeding 100 mg/L was confined to within ~80 m of the dredge areas. The greatest distance the sediment plume was predicted to travel was 670 m from Tamil (Figure 6-4). This maximum concentration was experience from a very short amount of time, before the plume dispersed.

For the windy period simulation (January to February 2020) the spatial extents of predicted impacts were very aligned with the calm period scenario; the model predicted the following:

- The **mean** distance ΔSSC exceeded 50 mg/L extended 30 m from the turning basin dredge site, while ΔSSC remained below 5 mg/L at the other dredging sites. At the disposal sites, the mean distance ΔSSC exceeded 5 mg/L extended up to 200 m, with the highest localized average concentrations predicted to exceed 100 mg/L at Rull (for a very short amount of time) (Figure 6-5).
- ΔSSC exceeding 5 mg/L was predicted to extend a **maximum** of 200 m from the edge of the dredging (Figure 6-6). The spatial extents of sediment plumes from the disposal sites were larger

than that from the dredging sites, extending a **maximum** of 50 m and 800 m (Figure 6-6 and Figure 6-7).

- ΔSSC greater than 50 mg/L was confined to the immediate vicinity of the dredging and disposal areas, occurring for very short periods of time. Disposal activities resulted in a ΔSSC greater than 50 mg/L occurring up to a maximum distance of 120 m from the stockpile site of Rull for 5% of the time (Figure 6-7).
- The maximum ΔSSC exceeding 100 mg/L was confined to within 80 m of the dredge areas. The greatest distance the sediment plume was predicted to travel was 670 m from Tamil, under windy conditions with no mitigation measures (i.e., silt curtains) (Figure 6-8). This maximum concentration was experienced from a very short amount of time, before the plume dispersed.

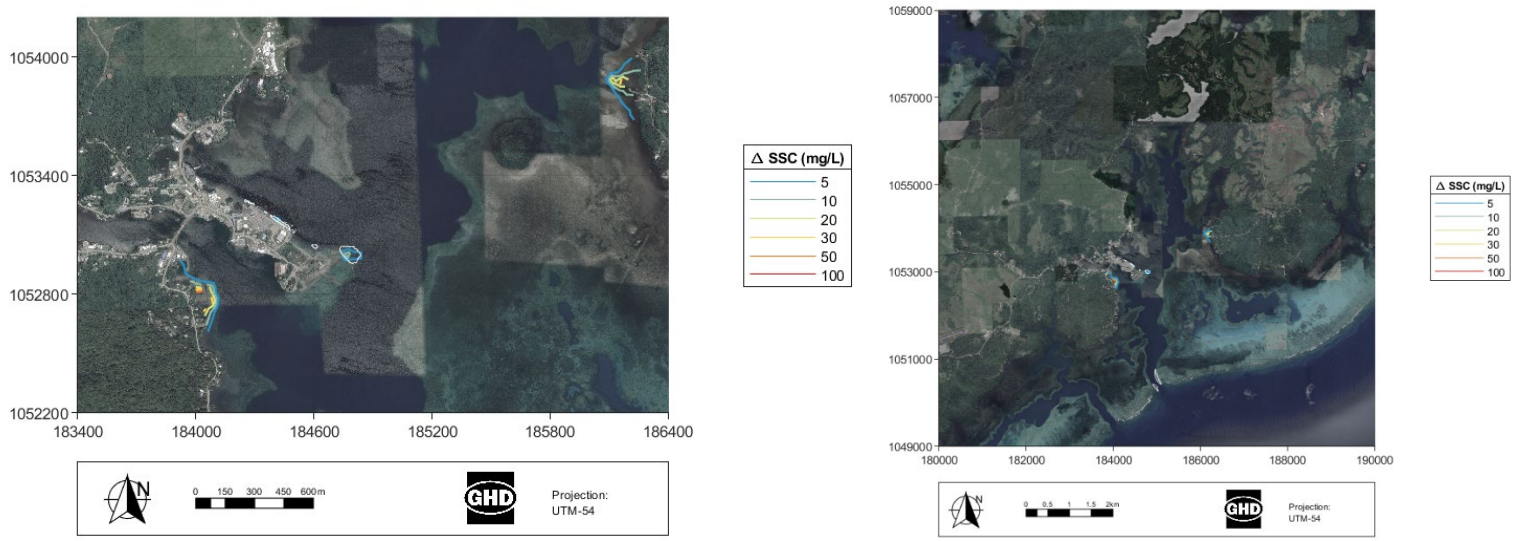

Figure 6-1 ***The mean ΔSSC for the calm scenario with site extent (left) and larger domain extent (right) for the Yap Port and surrounds***

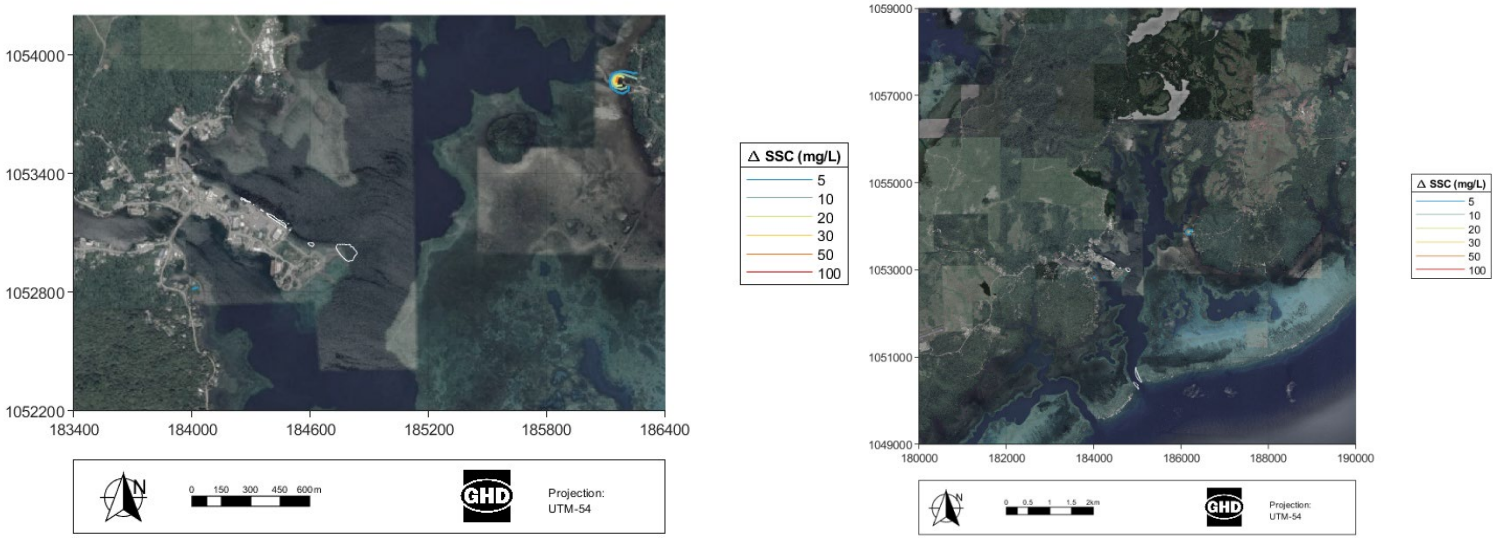

Figure 6-2 ***The 75th ΔSSC for the calm scenario with site extent (left) and larger domain extent (right) for the Yap Port and surrounds***

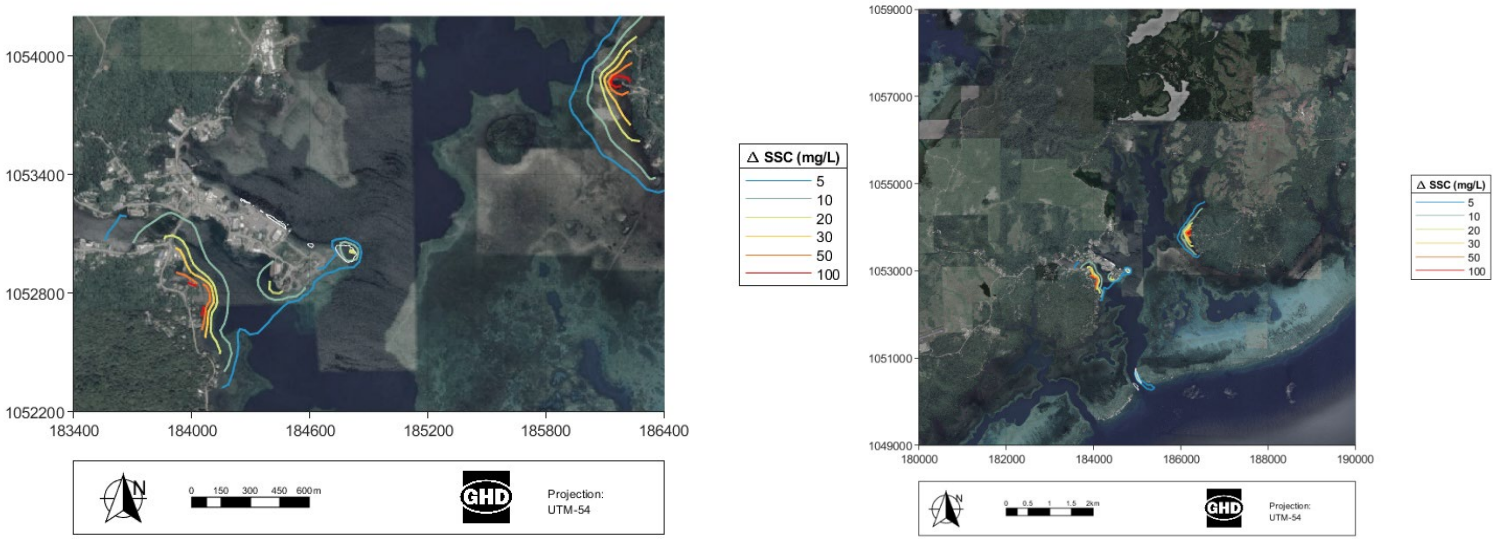

Figure 6-3 *The 95th ΔSSC for the calm scenario with site extent (left) and larger domain extent (right) for the Yap Port and surrounds*

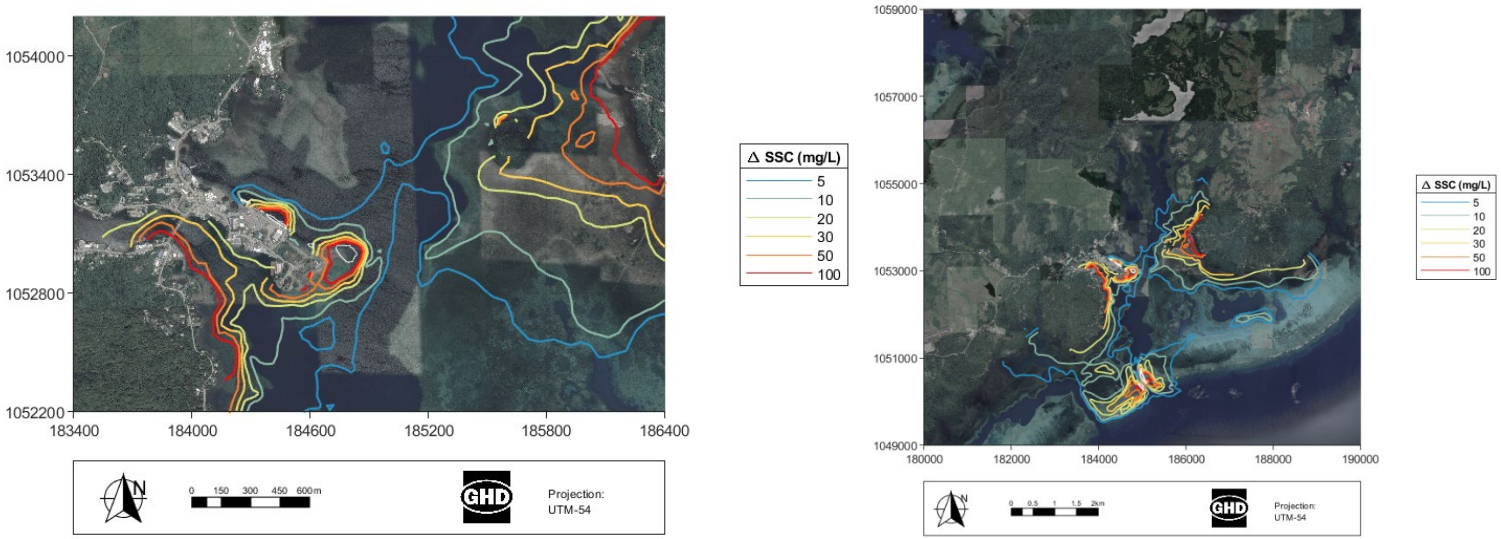

Figure 6-4 *The maximum ΔSSC for the calm scenario with site extent (left) and larger domain extent (right) for the Yap Port and surrounds*

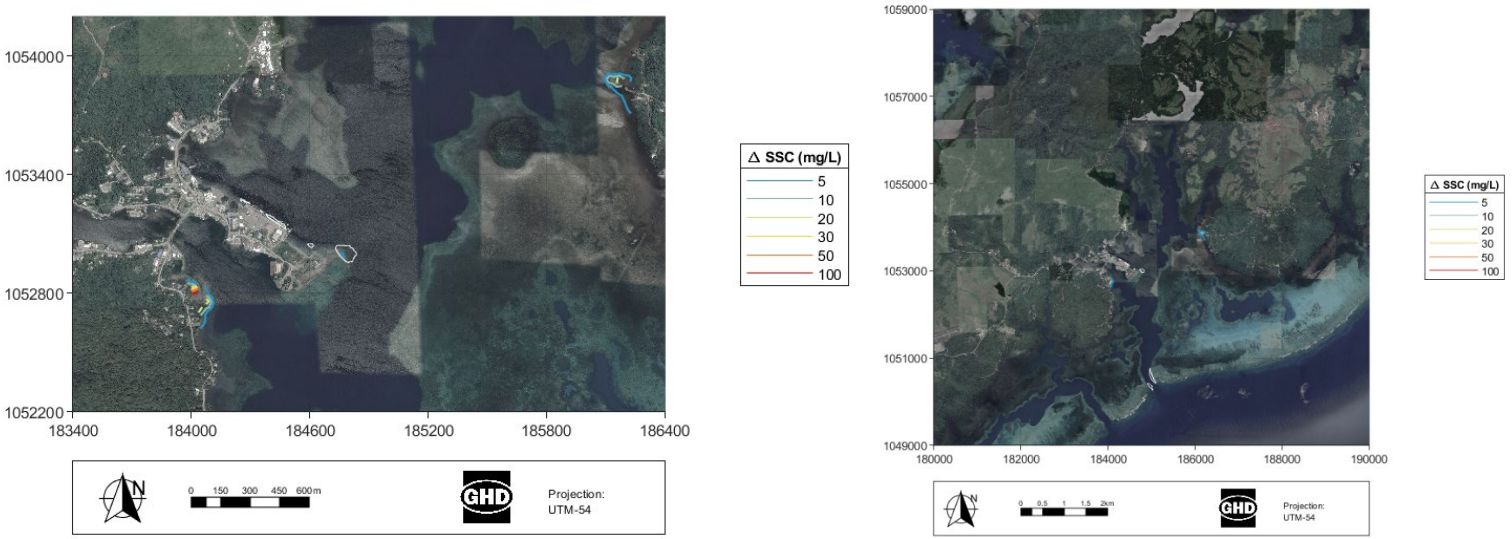

Figure 6-5 The mean ΔSSC for the windy scenario with site extent (left) and larger domain extent (right) for the Yap Port and surrounds

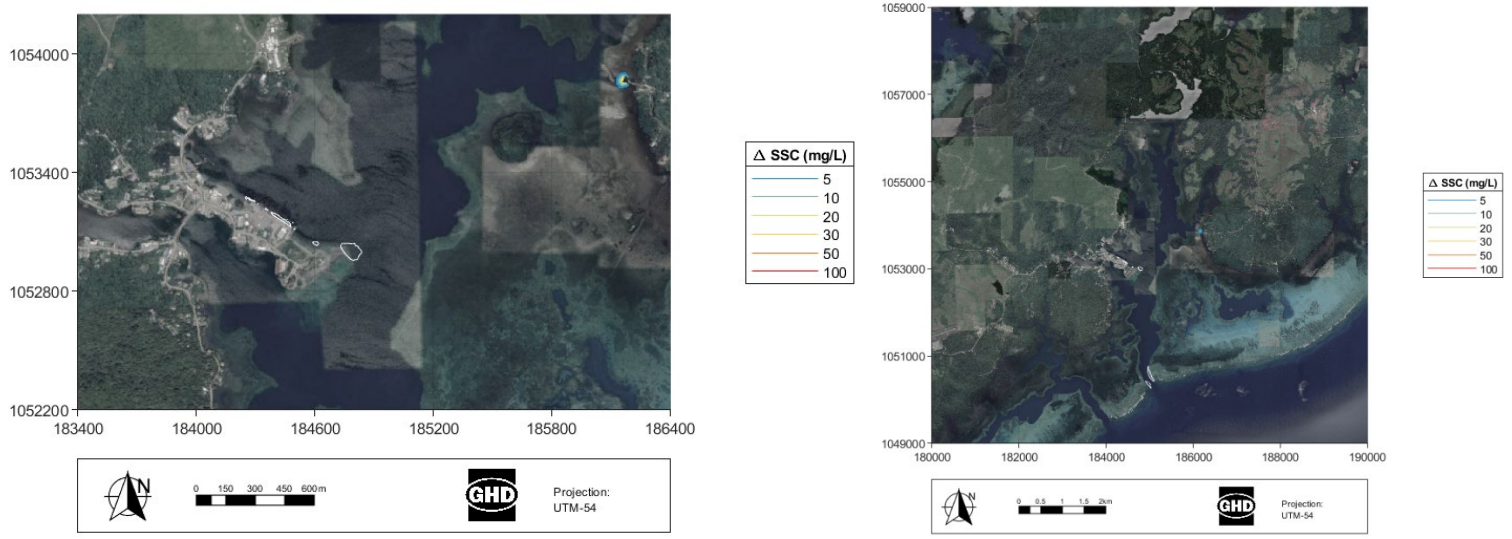

Figure 6-6 The 75th ΔSSC for the windy scenario with site extent (left) and larger domain extent (right) for the Yap Port and surrounds

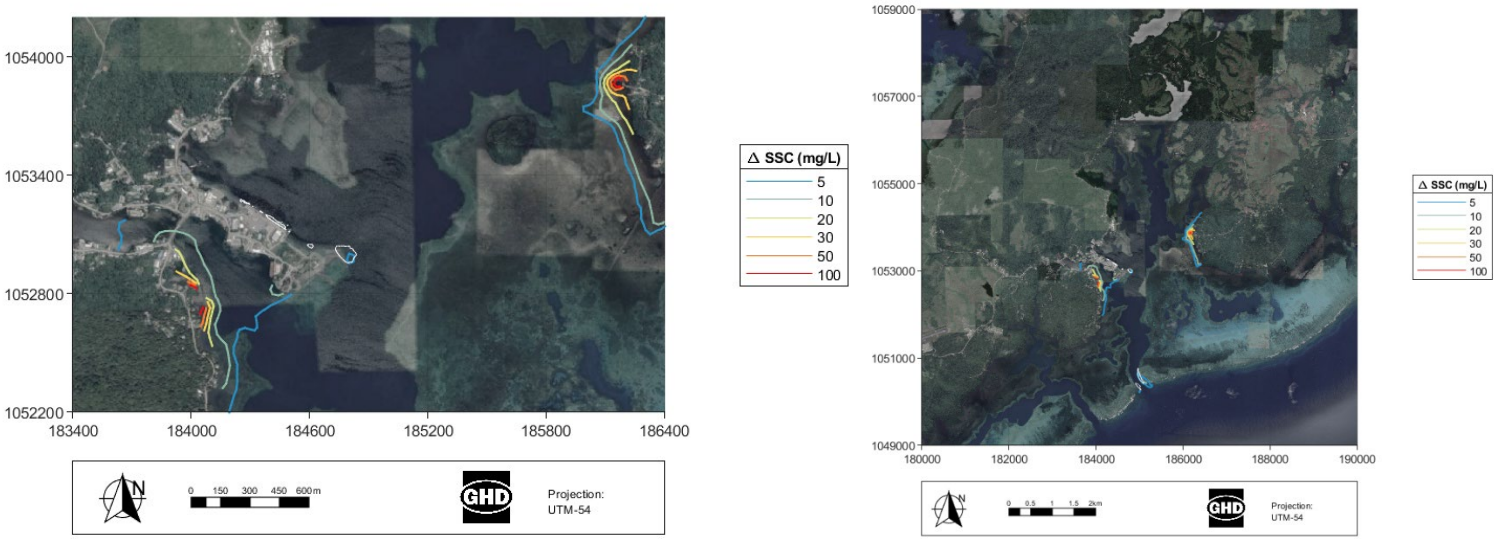

Figure 6-7 The 95th ΔSSC for the windy scenario with site extent (left) and larger domain extent (right) for the Yap Port and surrounds

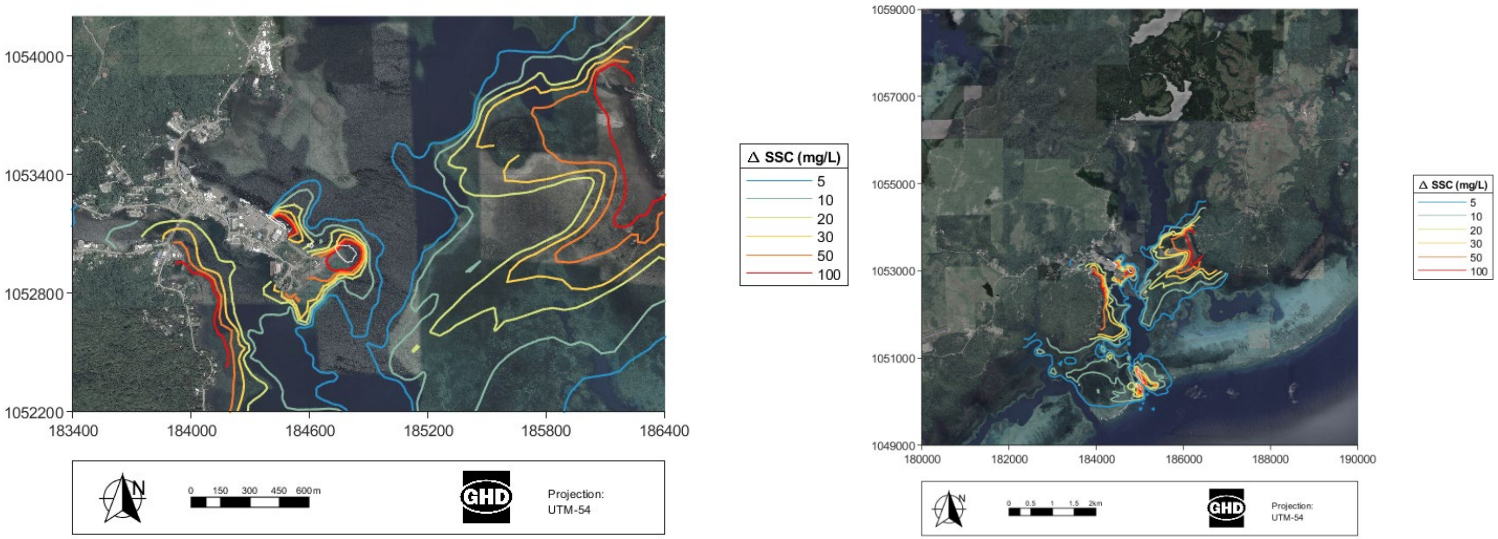

Figure 6-8 The maximum ΔSSC for the windy scenario with site extent (left) and larger domain extent (right) for the Yap Port and surrounds

6.1.2Time series SSC changes

The length of time elevated SSC are experienced is very important in the evaluation of impact, therefore a time series of concentrations were extracted under both windy and calm scenarios at the extraction locations was shown in Figure 6-9.

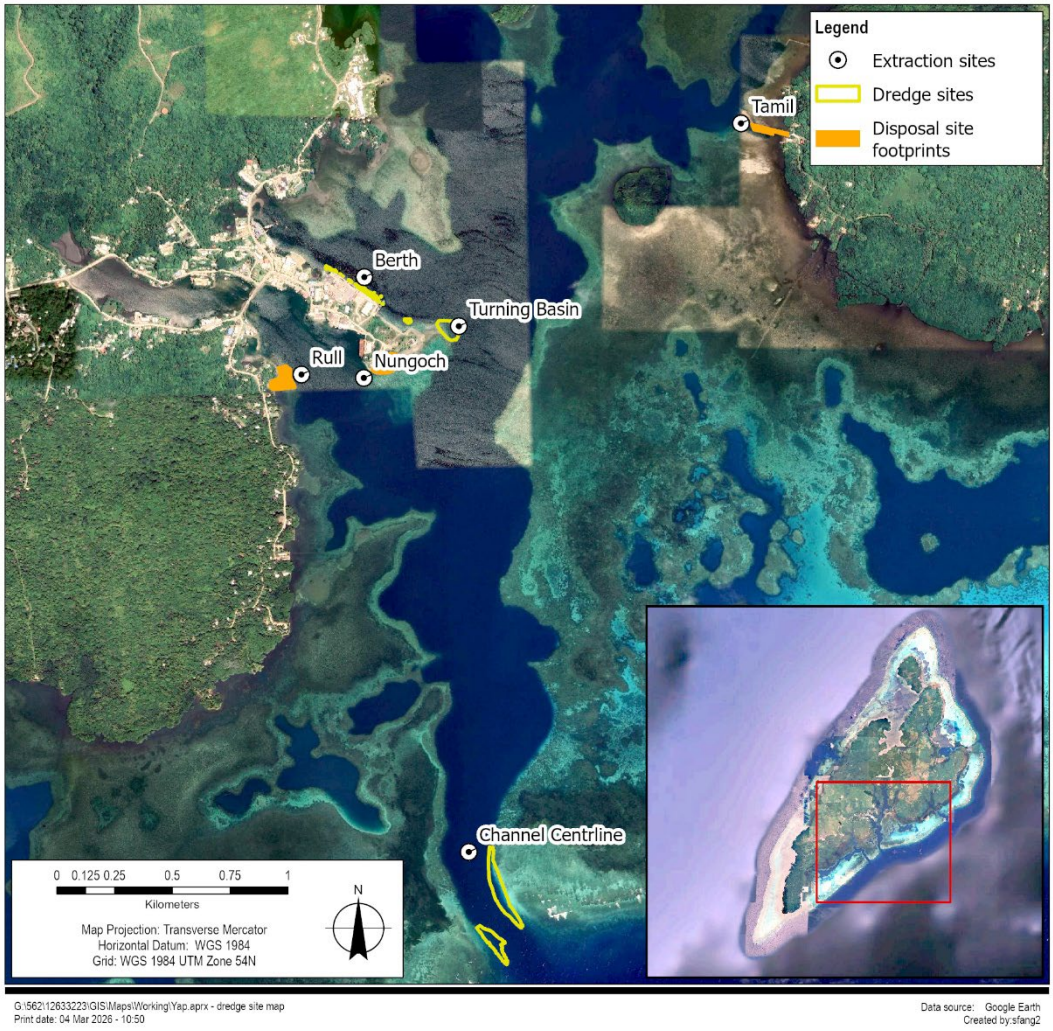

Figure 6-9 Extraction site for time series ΔSSC

The model predicted the following results, presented in Figure 6-10 and Figure 6-11.:

- ΔSSC increased primarily during active disposal and dredging periods for both scenarios, with the highest spikes occurring near the seabed during dredging at the turning basin.
- ΔSSC increased both at seabed and surface during disposal activities at each site (Rull, Tamil, and Nungoch).
- After the active dredging and disposal ceased at each site, both scenarios (calm and windy) showed a rapid return to low (or baseline) SSC levels (within a couple of hours).

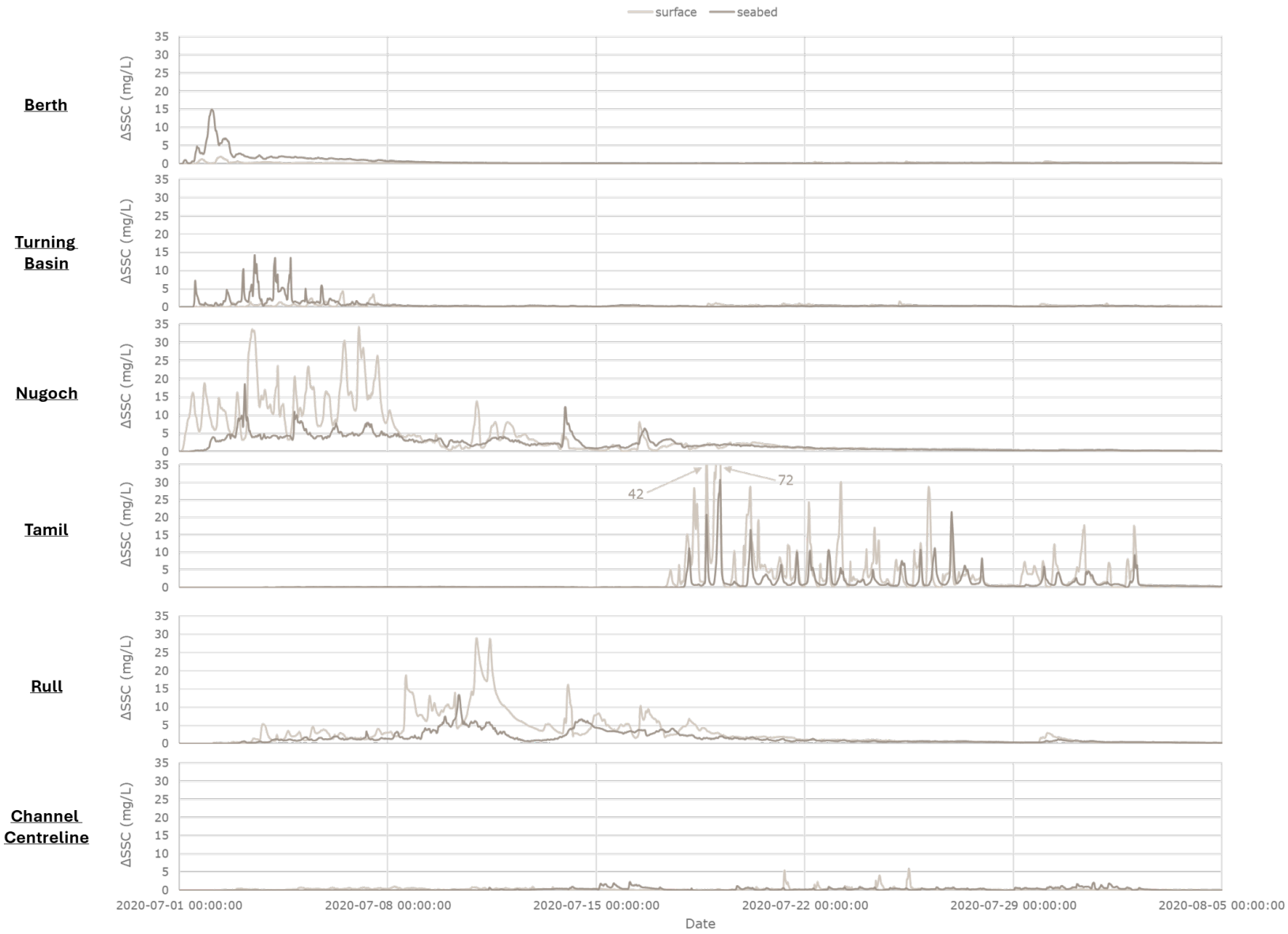

Figure 6-10 Time series ΔSSC for each sites during calm scenario

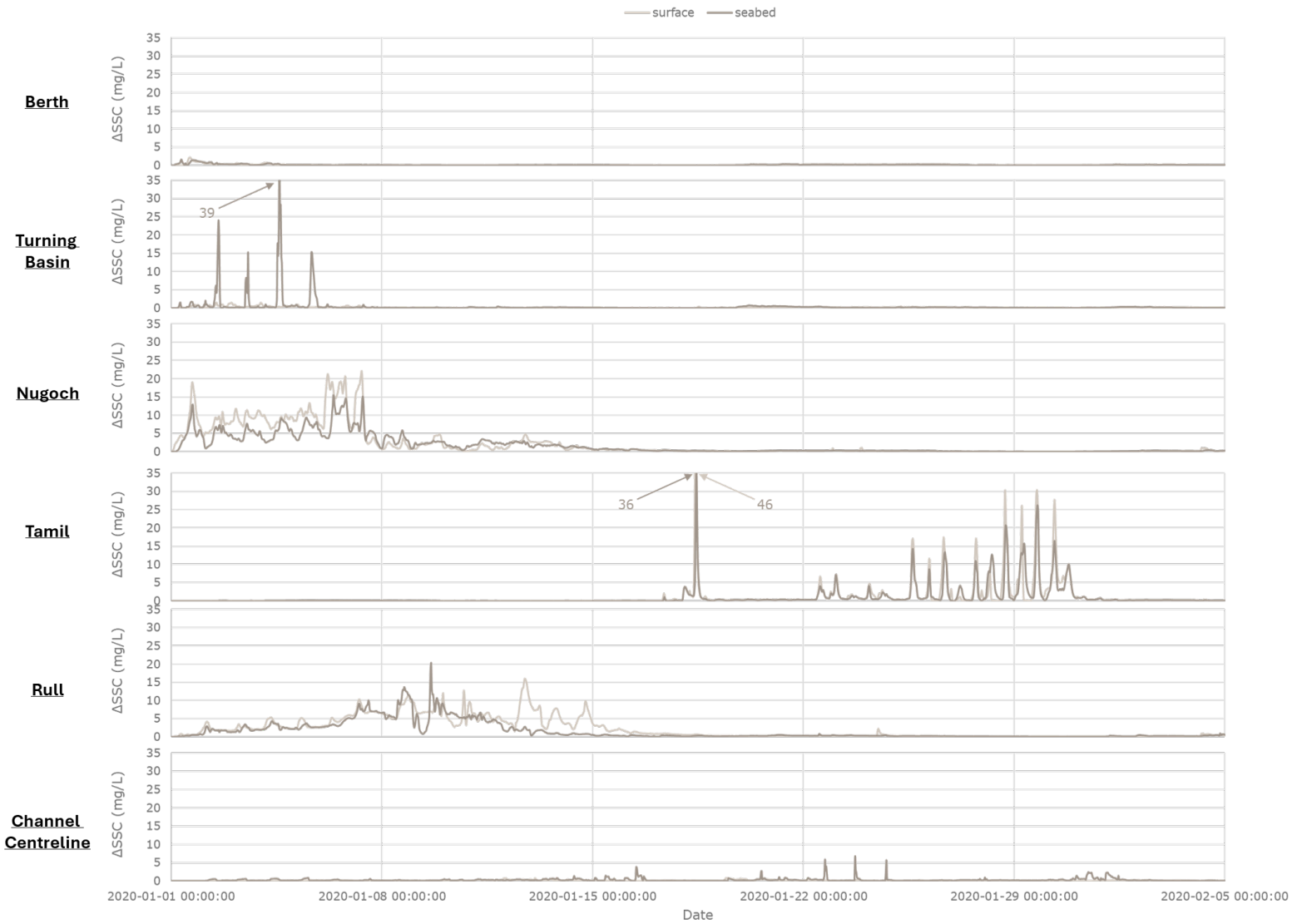

Figure 6-11 Time series ΔSSC for each sites during windy scenario

6.2 Deposition

Statistical contours of sediment deposition were produced for the calm and windy scenarios. The 5th percentile, 25th percentile, 50th percentile (median), mean, 75th percentile, 95th percentile and maximum deposition thicknesses are presented in Figure 6-12 – Figure 6-18.

Minimum deposition thickness was configured with deposition thicknesses of zero. In this manner, the simulations predict the dredging-induced deposition thickness only, and do not consider any additional deposition or erosion of ambient sediments within the marine environment.

The statistical plots of deposition thickness spatial distribution under both windy and calm scenarios show similar patterns, namely:

- Deposition exceeding 20 mm was predicted within the dredge area throughout the entire simulation period under both windy and calm scenarios (as shown in the maximum percentile plots in Figure 6-25 and Figure 6-18). Additionally, deposition thickness exceeding 20 mm extended to 60 m and 80 m from the disposal sites during the windy scenario for 50% of the time (Figure 6-21 and Figure 6-14).
- Greater deposition thicknesses were predicted to occur from sediments mobilized at the disposal sites compared with the dredging areas, due to the higher simulated sediment flux at these locations and the concentration of flux at a single point from each disposal site (representing the outflow point). In contrast, the dredging-related flux moved sequentially between multiple dredge areas throughout the simulation.
- The pattern of maximum deposition thickness under both scenarios was generally aligned, except that deposition occurred at a slightly higher level in the localized area of Rull under windy conditions. In addition, deposition did not exceed 5 mm beyond 100 m from the dredging areas under either calm or windy conditions (Figure 6-25 and Figure 6-18). The maximum deposition thickness was predicted to be 100 mm within 50 m under both conditions at the Tamil stockpile site; 30 mm within 50 m under calm conditions and within 30 m under windy conditions at the Rull stockpile site; and less than 5 mm under both conditions at the Nungoch stockpile site, due to the limited extent of in-water placement.

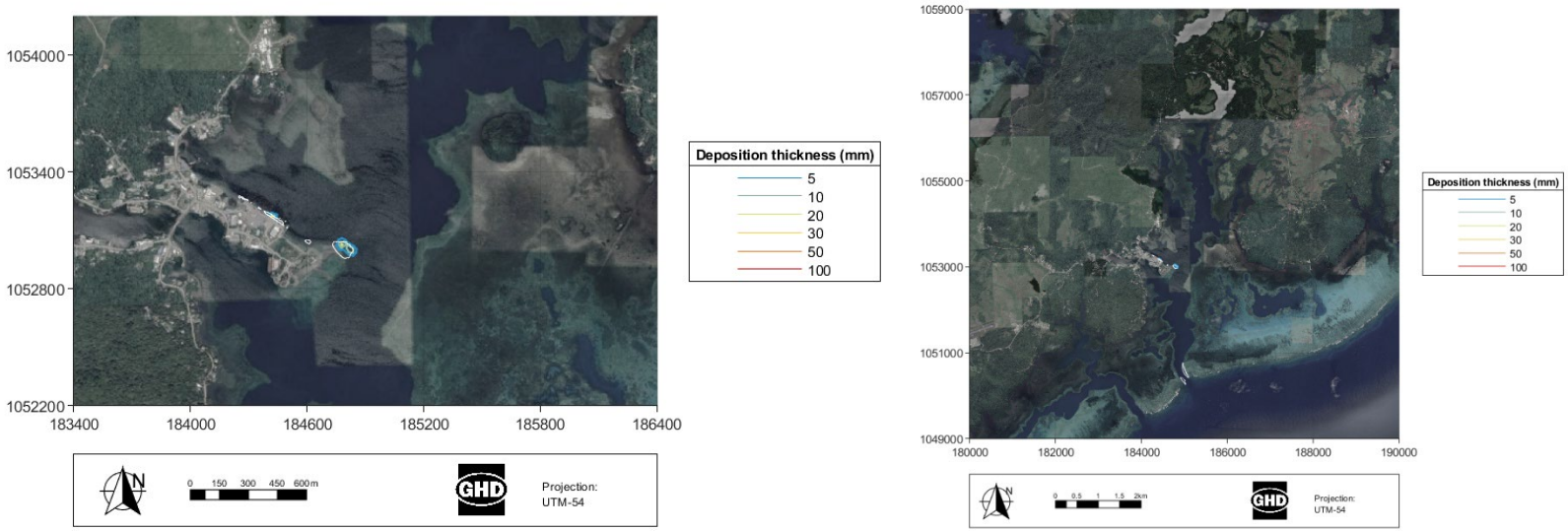

Figure 6-12 *5th percentile deposition thickness for the calm scenario with site extent (left) and larger domain extent (right) for the Yap Port and surrounds*

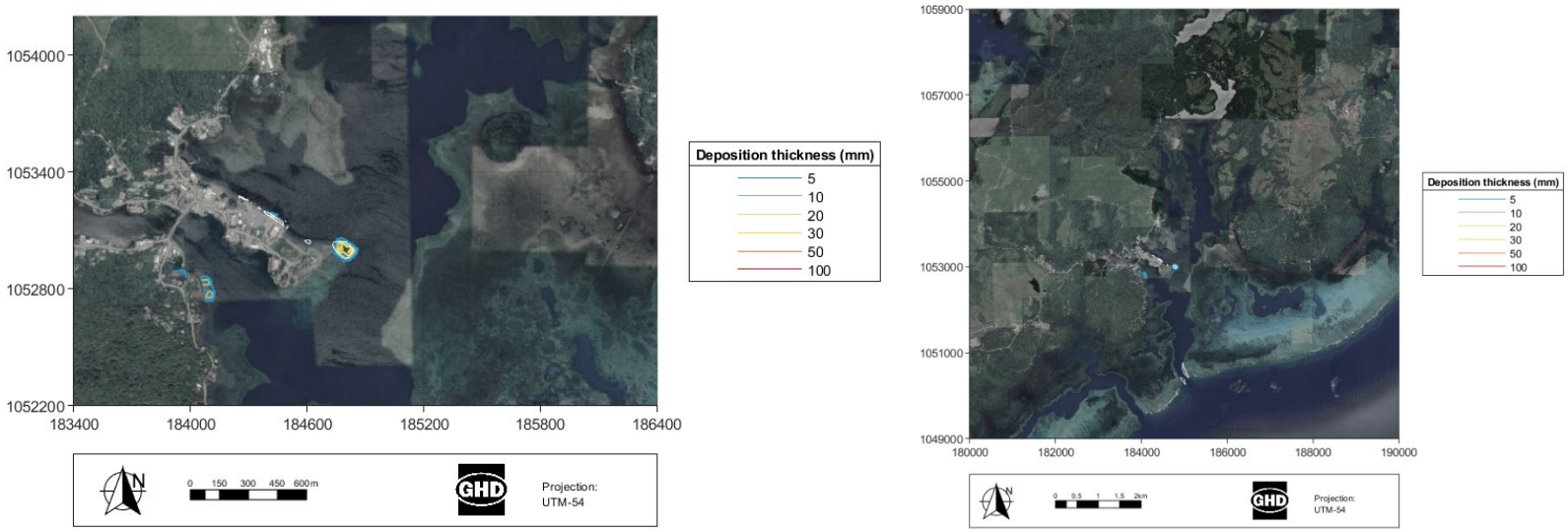

Figure 6-13 *25th percentile deposition thickness for the calm scenario with site extent (left) and larger domain extent (right) for the Yap Port and surrounds*

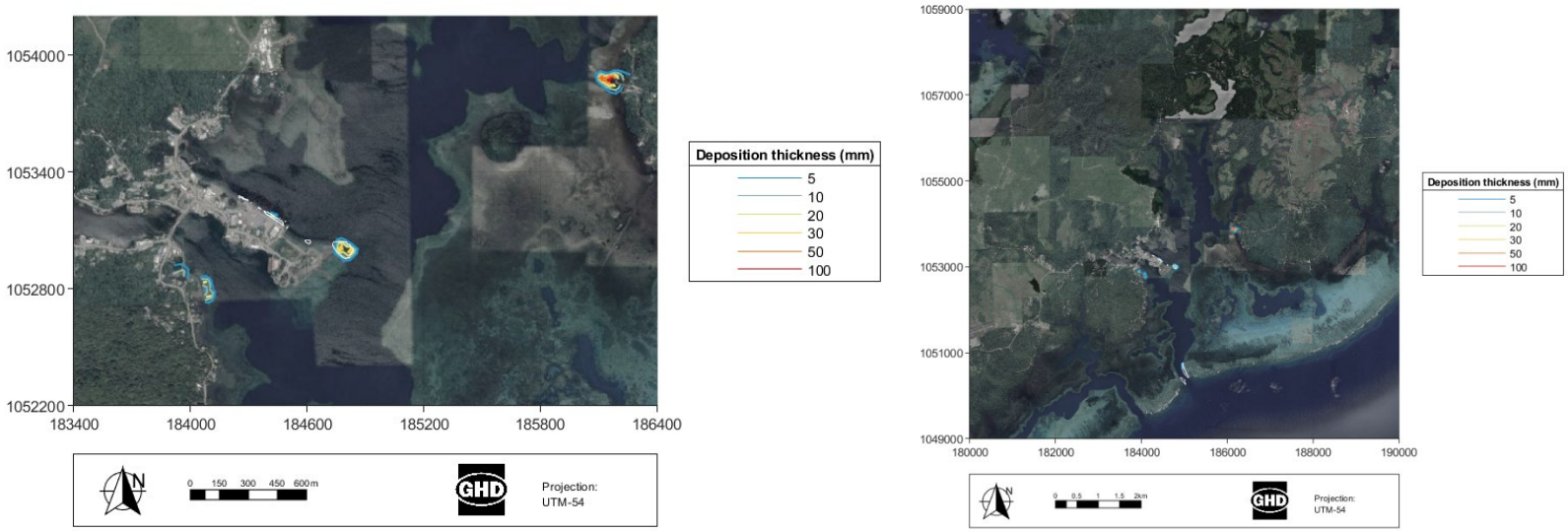

Figure 6-14 The median (50th percentile) deposition thickness for the calm scenario with site extent (left) and larger domain extent (right) for the Yap Port and surrounds

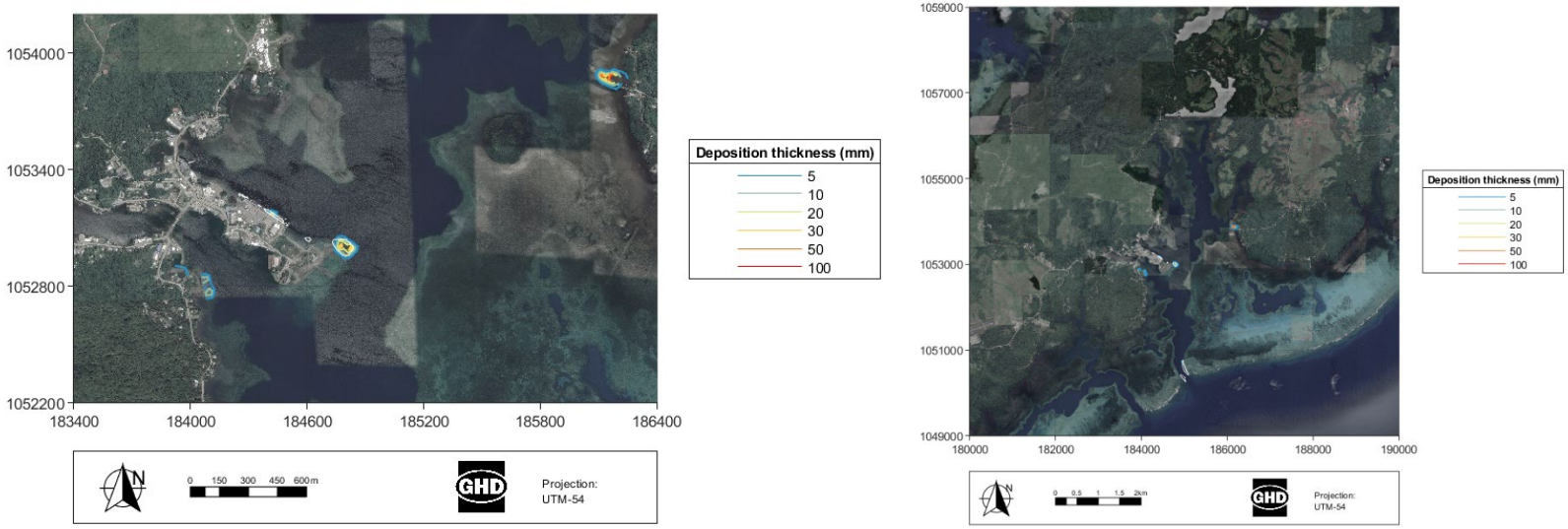

Figure 6-15 The mean deposition thickness for the calm scenario with site extent (left) and larger domain extent (right) for the Yap Port and surrounds

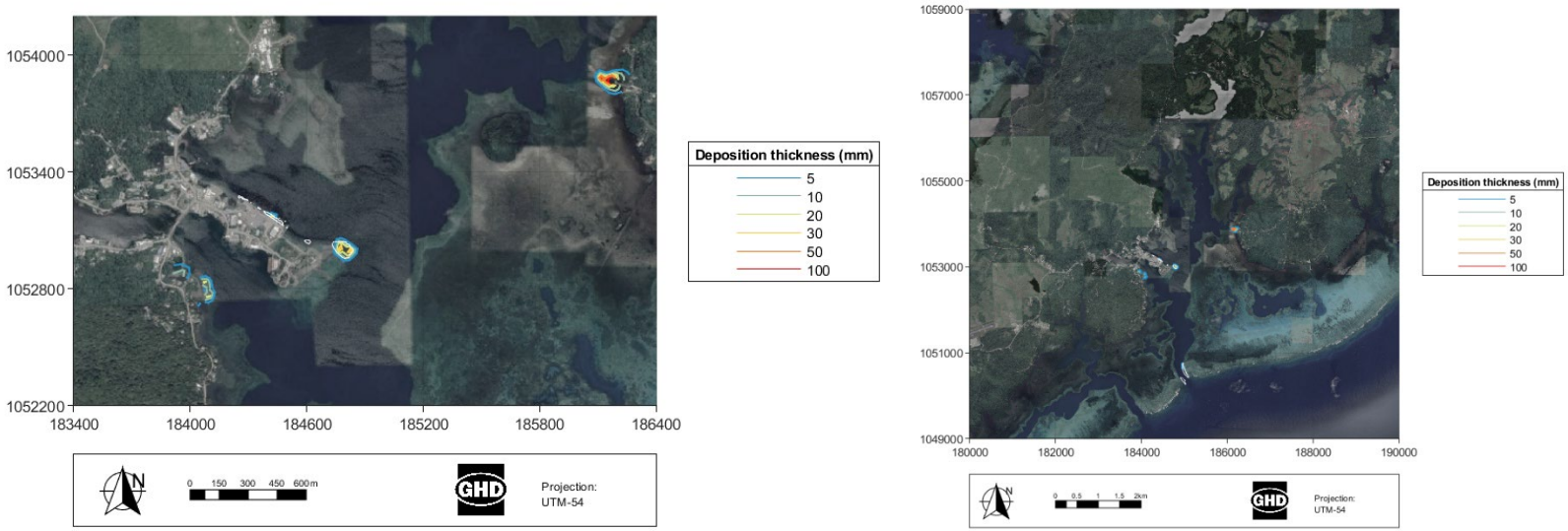

Figure 6-16 75th percentile deposition thickness for the calm scenario with site extent (left) and larger domain extent (right) for the Yap Port and surrounds

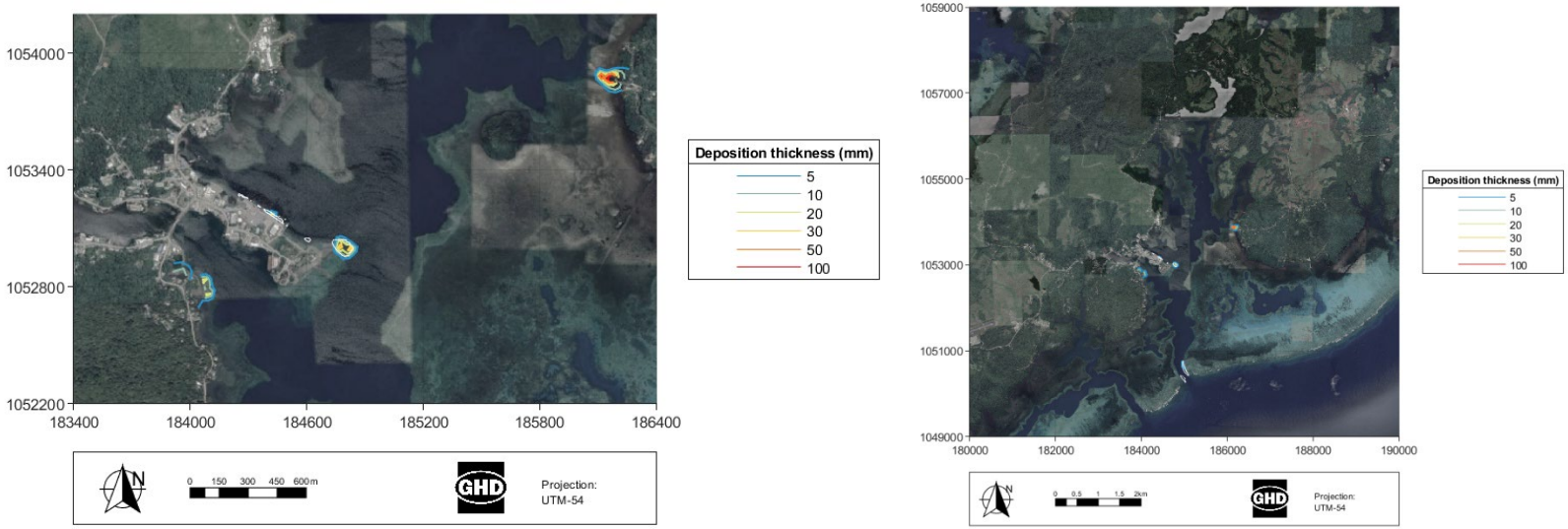

Figure 6-17 95th percentile deposition thickness for the calm scenario with site extent (left) and larger domain extent (right) for the Yap Port and surrounds

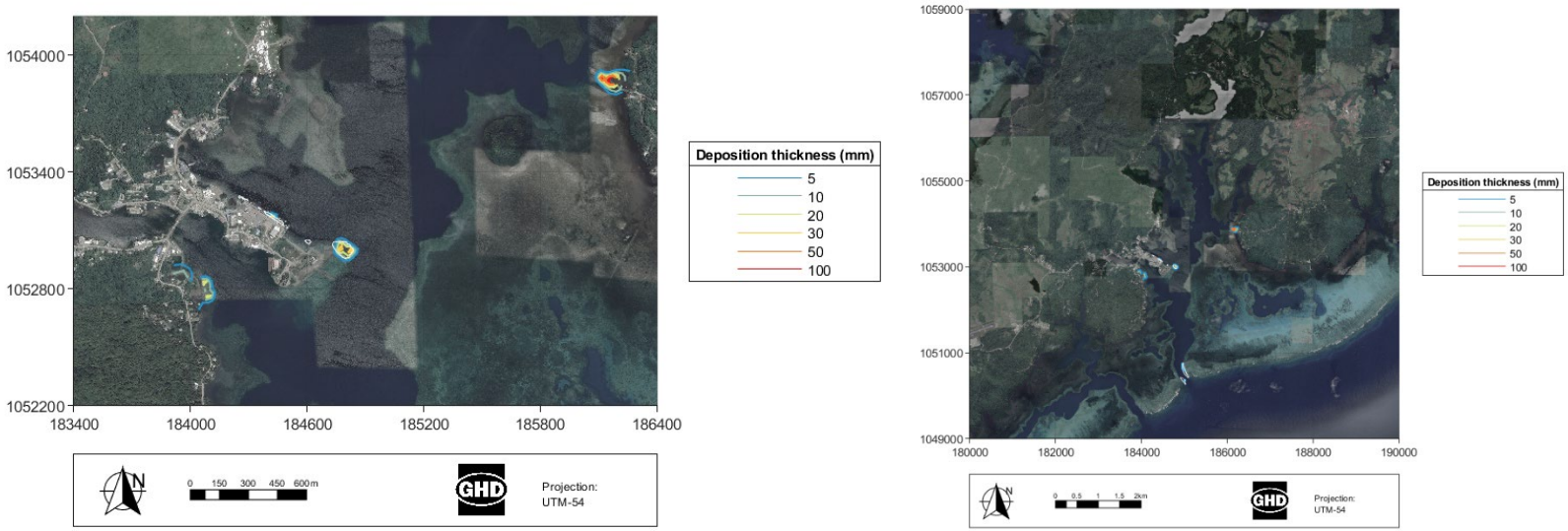

Figure 6-18 The maximum deposition thickness for the calm scenario with site extent (left) and larger domain extent (right) for the Yap Port and surrounds

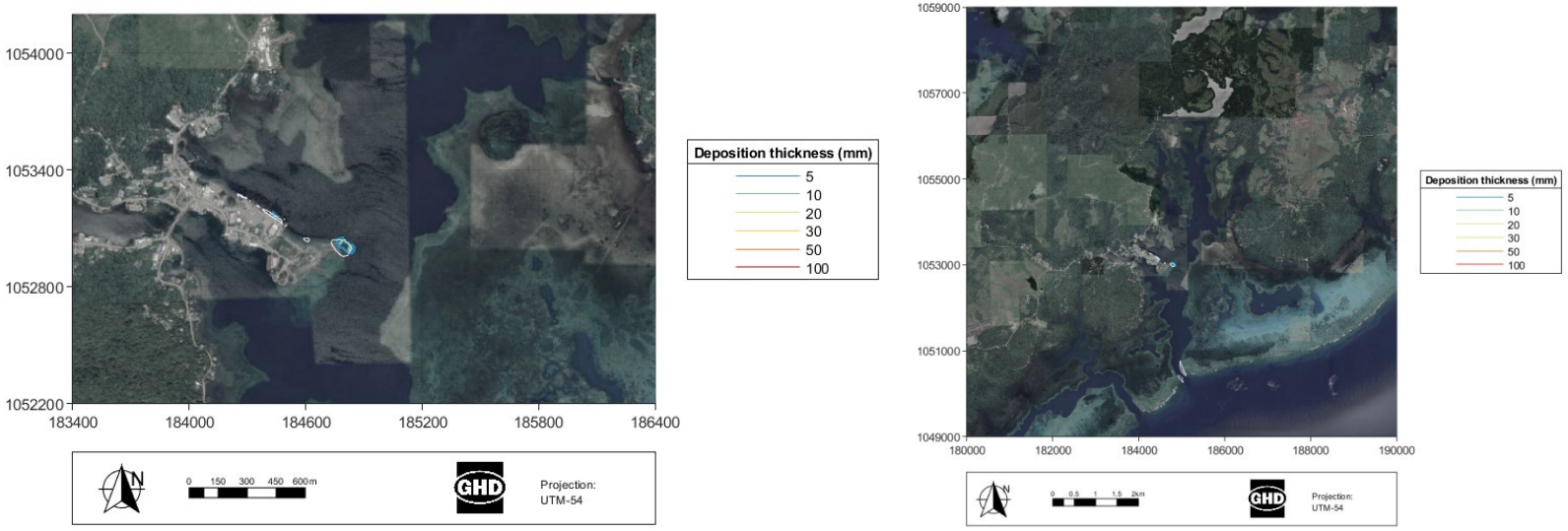

Figure 6-19 5th percentile deposition thickness for the windy scenario with site extent (left) and larger domain extent (right) for the Yap Port and surrounds

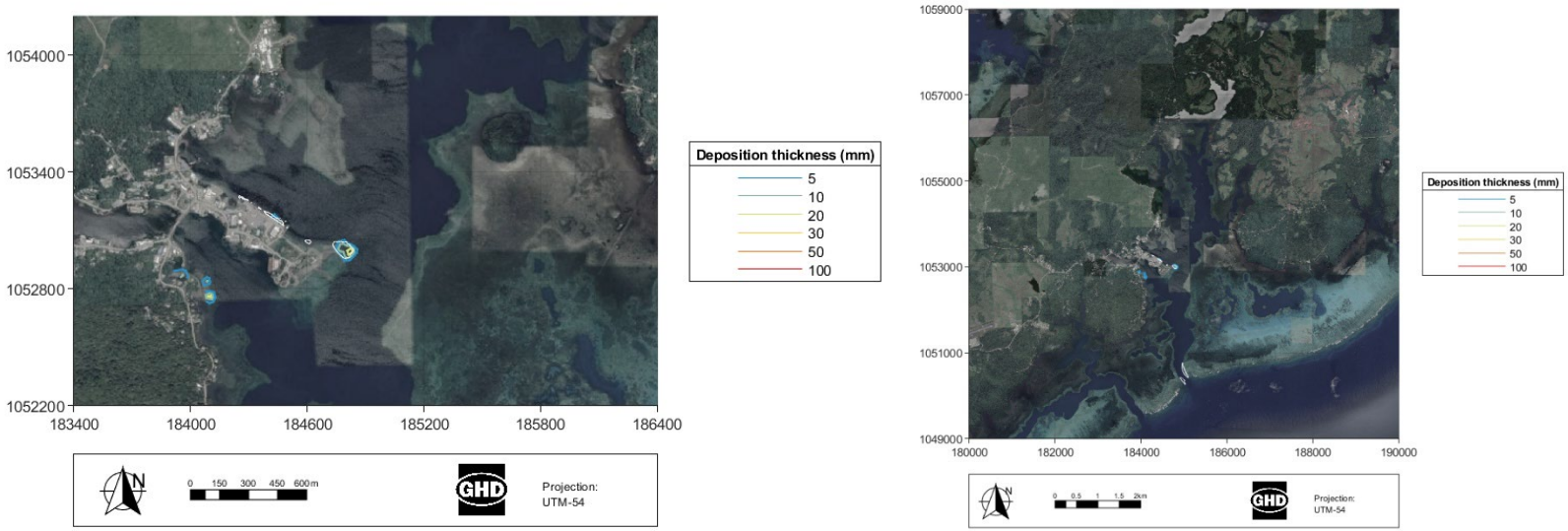

Figure 6-20 25th percentile deposition thickness for the windy scenario with site extent (left) and larger domain extent (right) for the Yap Port and surrounds

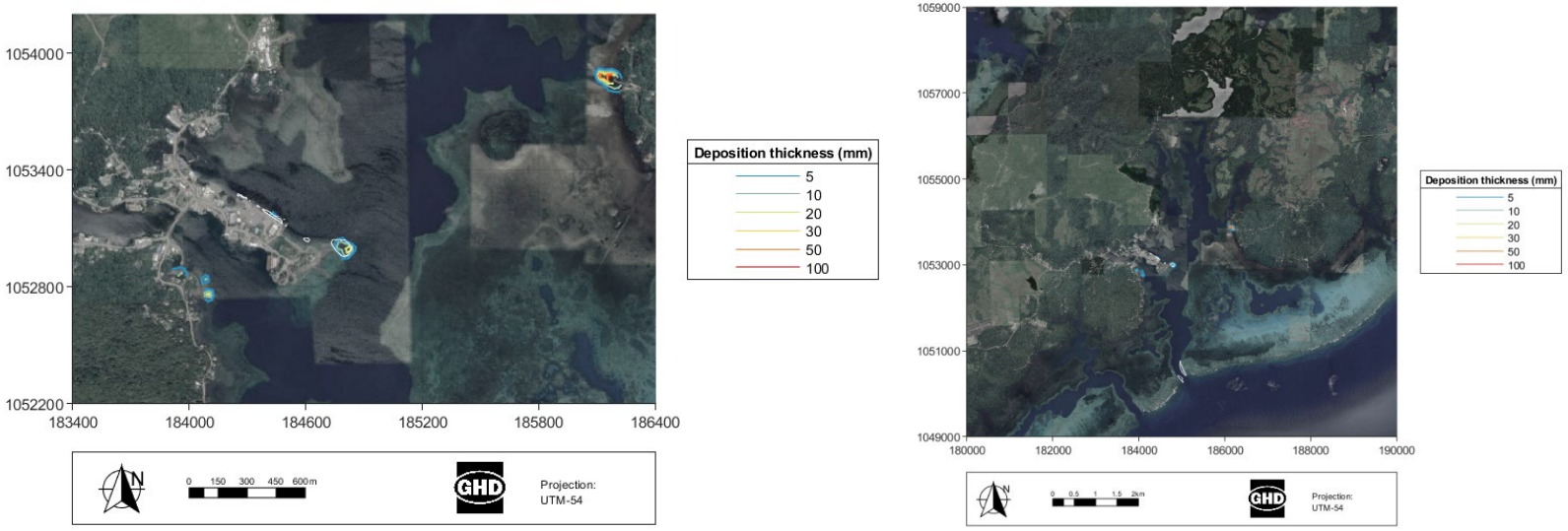

Figure 6-21 The median (50th percentile) deposition thickness for the windy scenario with site extent (left) and larger domain extent (right) for the Yap Port and surrounds

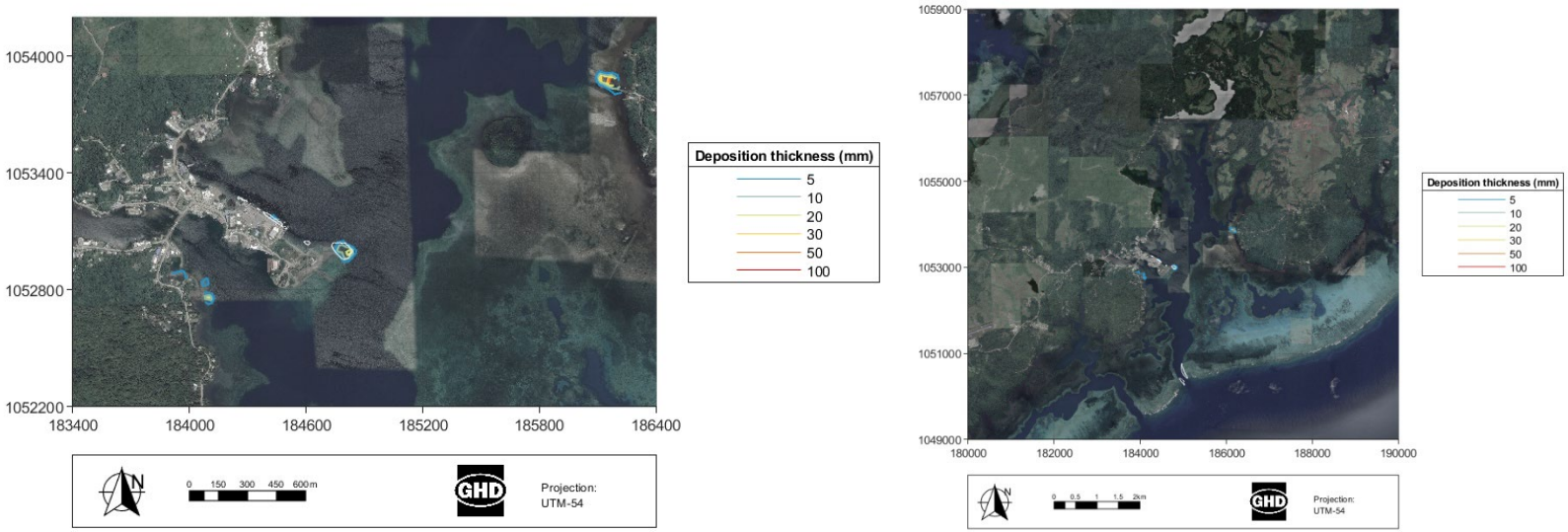

Figure 6-22 The mean deposition thickness for the windy scenario with site extent (left) and larger domain extent (right) for the Yap Port and surrounds

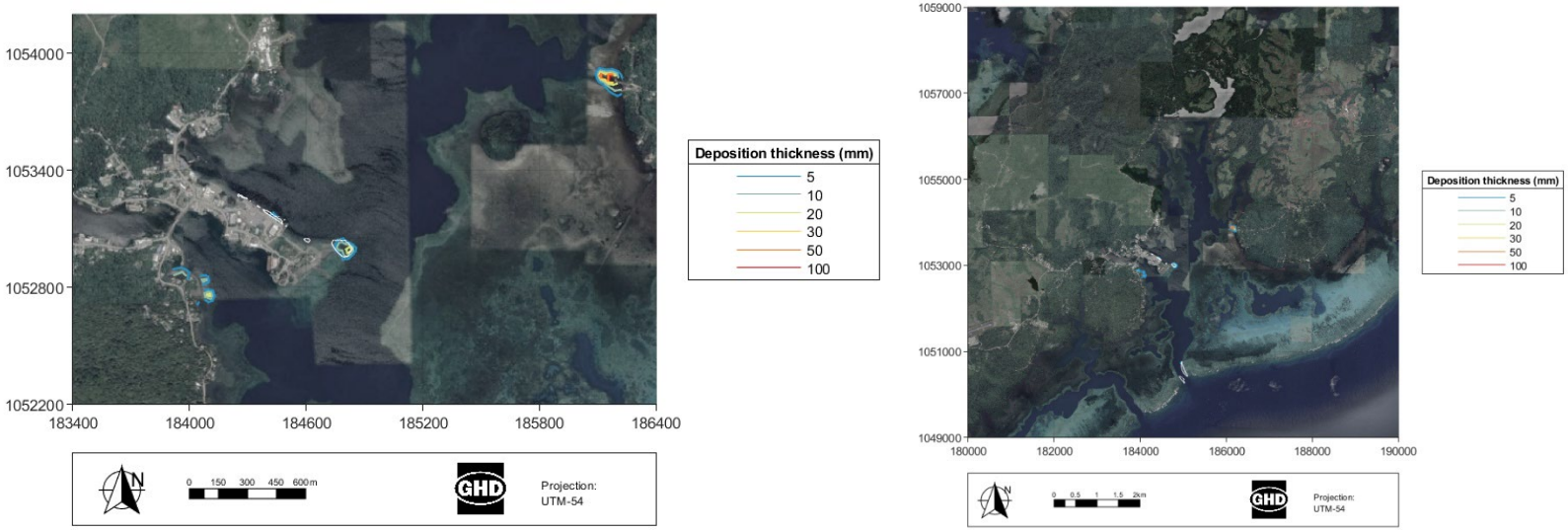

Figure 6-23 75th percentile deposition thickness for the windy scenario with site extent (left) and larger domain extent (right) for the Yap Port and surrounds

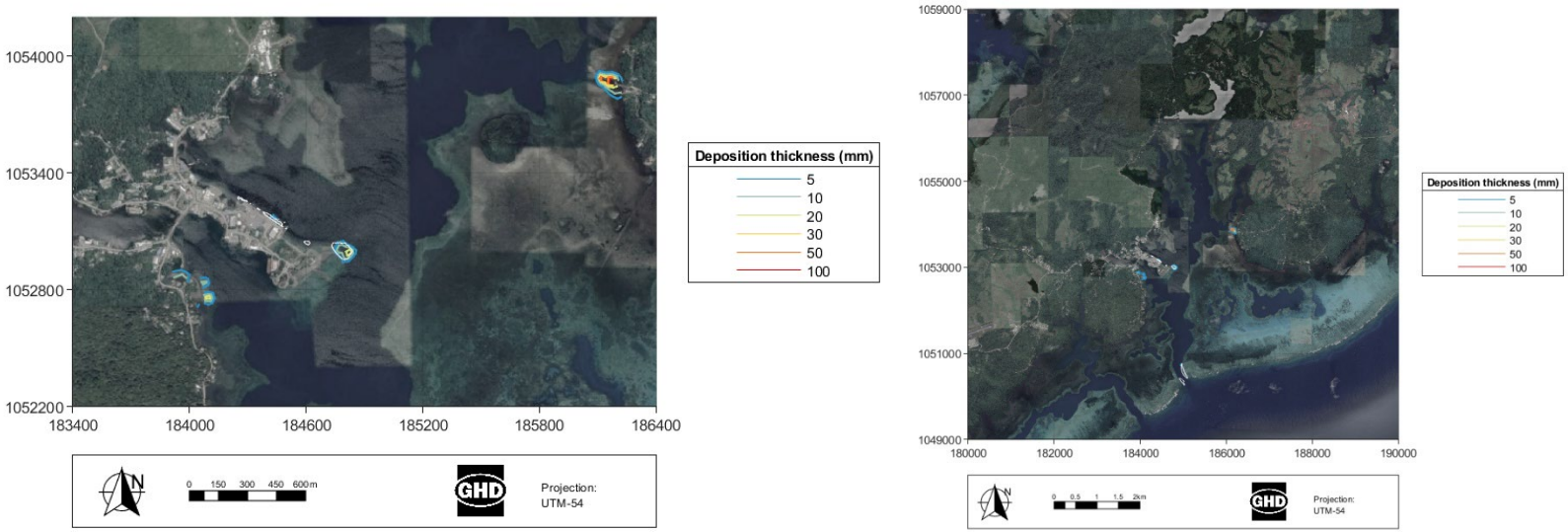

Figure 6-24 95th percentile deposition thickness for the windy scenario with site extent (left) and larger domain extent (right) for the Yap Port and surrounds

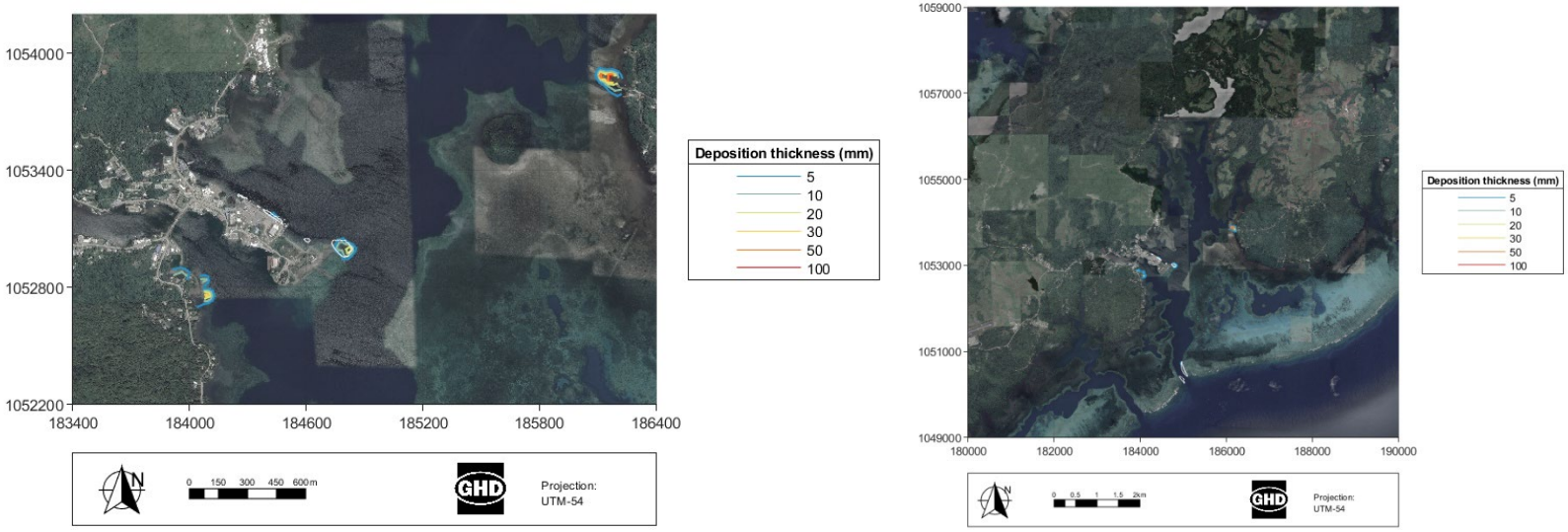

Figure 6-25 The maximum deposition thickness for the windy scenario with site extent (left) and larger domain extent (right) for the Yap Port and surrounds

7 Conclusions

A calibrated and validated 3D hydrodynamic model was used to simulate the fate and transport of sediments mobilized during the proposed Yap dredging and disposal activities. A representative year was selected from 30 years of global wave hindcast data. Within this year, two scenarios were modeled: windy conditions from January 1 to March 1, 2020, and calm conditions from July 1 to August 30, 2020. This seasonal differentiation enables a more robust assessment of plume dispersion under a range of environmental forcing conditions.

Sediment source terms were determined using the project dredging quantities, sampling data and conservative operational assumptions. The total in-situ dredge volume simulated was approximately 100,000 m³. Dredging was assumed to occur at an in-situ production rate of 200 m³/hr under a 24-hour operational schedule, 6.5 days/week, with 70% operational availability. These inputs yield a cumulative 31.6 calendar days of dredging activities. Input sediment flux estimates considered bucket drip fractions of 0.37 kg/s from large backhoe dredgers. Fine materials (clay and silt-sized particles) contributing to the far-field plume from the stockpile sites were modeled at an outflow of 0.10 kg/s. These assumptions present a high intensity dredging campaign resulting in conservative predictions, and do not represent any measure of mitigation such as the use of silt curtains.

A series of statistical plots showing the spatial extents of changes in SSC and deposition thickness were extracted. These were summarized using the 5th percentile, 25th percentile, 50th percentile (median), mean, 75th percentile, 95th percentile, and maximum values. The results of the modeling are summarized as follows:

- Under un-mitigated dredging and disposal, elevated suspended sediment concentrations are short-term and return to baseline quickly after activities cease.
- The un-mitigated maximum SSC are experienced for a very small percentage of time during activities, returning to baseline conditions within a couple of hours. Hence the significant difference in spatial extents between Mean and Max results.
- Calm vs Windy conditions have limited impact on suspended sediment trajectory.
- All modeling was un-mitigated, i.e., did not consider the use of silt curtains, which will confine the suspended sediments to inside the ‘mixing zone’ / limits of the curtains/barriers.
- The highest spikes in SSC occurred near the seabed during dredging, specifically at the turning basin (compared to the berth and entrance channel).
- Spikes in SSC occurred at the disposal sites at both the surface and the seabed, representative of water out-flow from the stockpiling activities.
- The maximum predicted deposition thickness, was 100 mm within 50 m at the Tamil stockpile site (calm and windy scenarios); 30 mm within 50 m under calm conditions and within 30 m under windy conditions at the Rull stockpile site; and <5 mm at the Nungoch stockpile site under both scenarios, with deposition not exceeding 5 mm beyond 100 m from the dredging areas.

8 References

Becker J, Eekelen Ev, Wiechen Jv, Lange Wd, Damsma T, Smolders T, and Koningsveld Mv (2015). Estimating source terms for far field dredge plume modelling. Journal of Environmental Management, Vol 149, pp 282-293.

Caldwell, P. C., M. A. Merrifield, P. R. Thompson (2015), Sea level measured by tide gauges from global oceans – the Joint Archive for Sea Level holdings (NCEI Accession 0019568), Version 5.5, NOAA National Centers for Environmental Information, Research Quality Dataset, doi: 10.7289/V5V40S7W.

Chassignet, E. P., Hurlburt, H. E., Smedstad, O. M., Halliwell, G. R., Hogan, P. J., Wallcraft, A. J., Baraille, R., & Bleck, R. (2007). The HYCOM (HYbrid Coordinate Ocean Model) data assimilative system. Journal of Marine Systems, 65(1–4), 60–8

Cheng, N. S. (1997). Simplified settling velocity formula for sediment particle. Journal of Hydraulic Engineering,123(2), 149-152.

Durrant, T., Greenslade, D., Hemer, M., & Trenham, C. (2014). A Global Wave Hindcast focussed on the Central and South Pacific. Melbourne: CAWCR.

Durrant, T., Hemer, M., Smith, G., Trenham, C., & Greenslade, D. (2019). CAWCR Wave Hindcast - Aggregated Collection. v5. CSIRO. Service Collection. Retrieved from http://hdl.handle.net/102.100.100/137152?index=1

Egbert, G. D., & Erofeeva, S. Y. (2002). Efficient inverse modeling of barotropic ocean tides. Journal of Atmospheric and Oceanic Technology, 19(2). https://doi.org/10.1175/1520-0426(2002)019<0183:EIMOBO>2.0.CO;2

GEOLABS (2025). Geotechnical data report Yap Wharf Improvements, 31 March 2025

GHD COWI (2024a). Dredging Strategy Report, Report produced by GHD Pty Ltd, 8 November 2024

GHD COWI (2024b). Dredging Disposal Plan, Report produced by GHD Pty Ltd, 8 November 2024

Hersbach, H., Bell, B., Berrisford , P., Biavati, G., Horányi, A., Muñoz Sabater, J., . . . Thépaut, J.-N. (2018). RA5 hourly data on single levels from 1940 to present. Copernicus Climate Change Service (C3S) Climate Data Store (CDS).

Willmott, CJ (1982) Some Comments on the Evaluation of Model Performance. Bulletin American Meteorological Society, Vol 63, No. 11, 1309-1313.

Willmott, CJ, SG Ackleson, RE Davis, JJ Feddema, KM Klink, DR Legates and CM Rowe (1985) Statistics for the Evaluation and Comparison of Models. Journal of Geophysical Research, Vol 90, No. C5, 8995-9005.